

**The role of surface modification on zirconia implants to
enhance osteoblasts adhesion and proliferation**

**Inaugural-Dissertation
zur Erlangung des Doktorgrades
der Zahnheilkunde**

**der Medizinischen Fakultät
der Eberhard-Karls-Universität
zu Tübingen**

vorgelegt von

Al-Qahtani Waleed

2014

Dekan: Professor Dr.B. Autenrieth

1.Berichterstatter: Professor Dr.J.Geis-Gerstorfer

2.Berichterstatter: Professor Dr.Dr. M.Krimmel

Table of content.....	I
List of Tabela.....	III
List of figures.....	IV
List of abbreviations.....	VI
1.0 Introduction	1
1.1 Implant material concept.....	1
1.2 Zirconia	2
1.3 Physical properties of zirconia	4
1.4 Form and microstructure of zirconia	5
1.5 Surface roughness.....	6
1.6 Cellular adhesion	10
1.7 Aim of the study	12
2.0 Material and methods	13
2.1 Sample preparation.....	14
2.1.1 Zirconia disc preparation.....	14
2.1.2 Titanium disc preparation.....	15
2.1.3 Sandblasting and surface roughness of zirconia samples.....	15
2.1.4 Preparing the zirconia samples for measurement of surface topography..	16
2.2 Analysis of surface topography before sintering	16
2.3 Sintering process	17
2.4 Analysis of surface topography after sintering.....	18
2.5 Cleaning the samples and preparation for biological tests	18
2.6 Biological tests.....	19
2.6.1 Osteoblast cell culture.....	19
2.6.2 Crystal violet test of adhesion and cell coverage.....	20
2.6.3 Crystal violet test of initial adhesion.....	20
2.6.4 Crystal violet test of cell coverage	21
2.6.5 Test of metabolic activity and proliferation.....	22
2.6.5.1 Principle of the XTT assay	22
2.6.5.2 Principle of the BrdU proliferation test	22
2.6.5.3 XTT and BrdU procedures.....	23
2.7 Data analysis	24
2.7.1 Data analysis of surface topography and roughness.....	24

2.7.2 Data analysis for cell adhesion and cell spreading	25
2.7.3 Data analysis of metabolic activity (XTT) and proliferation (BrdU)	25
3.0 Results	26
3.1 Surface roughness and topography	26
3.1.1 Surface roughness	26
3.1.2 Topography	28
3.2 Adhesion and cell coverage	34
3.2.1 Adhesion test	35
3.2.2 Cell spreading and coverage	38
3.3 Test of metabolic activity and proliferation	41
3.3.1 Metabolic activity (XTT assay)	41
3.3.2 Proliferation test (BrdU assay)	43
4.0 Discussion	45
4.1 Surface topography and roughness	45
4.2 Cell culture model	47
4.3 Effect of surface modification on cellular adhesion, spreading, metabolic activity, and proliferation	48
4.3.1 Cell adhesion and cell coverage (crystal violet assay)	48
4.3.2 Metabolic activity (XTT assay)	49
4.3.3 Cell proliferation (BrdU assay)	49
5.0 Conclusions and outlook	52
6.0 Summary	53
7.0 Literature	54
8.0 Appendix	60
8.1 Results of surface roughness in the actual test	60
Acknowledgment	66
Curriculum vitea	67

List of Tabela

Table 1: Properties of zirconia	4
Table 2: Summarized table from a study by Gahlert et al. illustrating the surface roughness of different materials	7
Table 3: Topographic and removal torque of the implants used in animal experimentation by Gahlert et al. (2007)	8
Table 4: Techniques to roughen zirconia surfaces by sandblasting	9
Table 5: Surface design of some commercially available zirconia implants	10
Table 6: Surface analysis of zirconia	27
Table 7: Surface roughness of 10 randomized samples out of 50 samples of machined zirconia before the sintering procedure.....	60
Table 8: Surface roughness of 10 randomized samples out of 50 samples of machined zirconia after the sintering procedure	61
Table 9: Surface roughness of 10 randomized samples out of 50 samples of 120 μm sandblasted zirconia before the sintering procedure	62
Table 10: Surface roughness of 10 randomized samples out of 50 samples of 120 μm sandblasted zirconia after the sintering procedure	63
Table 11: Surface roughness of 10 randomized samples out of 50 samples of 250 μm sandblasted zirconia before the sintering procedure	64
Table 12: Surface roughness of 10 randomized samples out of 50 samples of 250 μm sandblasted zirconia after the sintering procedure	65

List of figures

Figure 1: The Tübingen Immediate Implant (Tübinger Sofortimplantat).....	2
Figure 2: A titanium implant and a metal-free zirconia implant.	3
Figure 3: Zirconia phase transformation	5
Figure 4: Study outline.....	13
Figure 5: Production of zirconia samples using a cutting machine.....	14
Figure 6: The tool used to control	15
Figure 7: Perthometer used, to analysis surface roughness of samples.....	17
Figure 8: Sintering machine for sandblasted samples	18
Figure 9: Example of a crystal violet test.....	21
Figure 10: Average surface roughness of zirconia samples \pm SD.....	27
Figure 11: Scanning electron microscopy of different sintered zirconia samples and titanium.....	28
Figure 12: D-Profile of sandblasted zirconia samples before and after sintering	29
Figure 13: D-Profile of 10 machined zirconia samples before and after sintering	30
Figure 13: Surface roughness of a) a zirconia disc sandblasted with 250 μm Al_2O_3 before and b) after the sintering process.	31
Figure 14: Surface roughness of a) a zirconia disc sandblasted with 120 μm Al_2O_3 before and b) after the sintering process..	32
Figure 15: Surface roughness of a) a machined polished zirconia disc before and b) after the sintering process.....	33
Figure 16: Surface roughness of a smooth titanium samples.....	34
Figure 18: Initial cell adhesion of SAOS-2 osteoblasts after 1 h.	35
Figure 19: Initial cell adhesion after 1 h. The means of three experiments	36

Figure 20: SEM of intial adhesion of osteoblast on various surfaces.	37
Figure 21: Surface coverage of SAOS-2 osteoblast cells after 72 h.	38
Figure 22: Test of cell coverage by crystal violet. The means of three experiments.....	39
Figure 23: Photo documentation of Crystal violet test after 72 h	40
Figure 24: Metabolic activity of osteoblasts after 48 h.	41
Figure 25: XTT assay. The results of three experiments are summarized	42
Figure 26: Osteoblast proliferation test after 24-48 h. A typical experiment.....	43
Figure 27: BrdU assay. The results of three experiments are summarized	44

List of abbreviations

Al₂O₃: Aluminum oxide

ATZ: Alumina-toughened zirconia

BIC: Bone implant contact

BrdU: Bromo-deoxy-uridine

CaO: Calcium oxide

EDTA: Ethylenediaminetetraacetic acid

ELISA: Enzyme linked immunosorbent assay

FCS: Fetal calf serum

HRP: Horseradish peroxidase-conjugated goat anti-mouse

HV: Vickers hardness

MPa: Megapascals

MTT: (3-[4,5-Dimethylthiazol-2-yl]-2,5 diphenyl tetrazolium bromide)

PBS: Phosphate buffered saline

PSZ: Partially stabilized zirconia

Pt: Profile's depth

RTQ: Removal torque

Ra: Average roughness

Rz: Roughness

Rmax: Maximum surface roughness

SEM: Scanning electron microscope

TiO₂: Titanium dioxide

TPS: Titanium plasma-sprayed

TZP: Tetragonal zirconia polycrystal

XTT: (2,3-Bis- (2-methoxy-4-nitro-5-sulfophenyl)-2*H*-tetrazolium-5-carboxanilide)

Y-TZP: Yttria-stabilized TZP

Y₂O₃: Yttria

ZrO₂: Zirconia

1.0 Introduction

1.1 Implant material concept

The present material of choice for dental implants is commercially pure titanium (degree 1-4 ASTM). The mechanical and biological features of titanium have been well documented and shown to be satisfactory (Adell et al. 1990). This material has been used for about 30 years as an implant substrate with high rates of success (Kasemo and Lausmaa 1988). However; the grayish color of titanium might show through thin mucosa (Fig. 2), which is an aesthetic drawback (Heydecke, Kohal, and Gläser 1999). Furthermore, over time the implant head may become visible because of peri-implant soft tissue recession. A case report demonstrated sporadic cases of Ti intolerance using MELISA testing, which evaluates lymphocyte proliferation (Oliva 2010).

Thus, there is increasing demand for metal-free implants. One possible solution would be to make implants from tooth-colored material, such as ceramic. Ceramic materials are highly biocompatible and can be used as dental devices (Silva, Lameiras, and Lobato 2002). One ceramic material that has been used for dental implants is aluminum oxide (Al_2O_3 ; Fig. 1) (Schulte 1984; De Wijs et al. 1994). This material osseointegrates well but does not have sufficient mechanical strength for long-term loading. Therefore, Al_2O_3 implants were withdrawn from the market.

Zirconia, another ceramic material with potential use as a dental implant, was introduced recently. This material clearly provides the highest quality aesthetics (Heydecke et al. 1999). Kohal and Klaus (2004) reported excellent aesthetics in a patient who received a machined zirconia implant and a zirconia crown. In addition to the aesthetic quality of zirconia, optimal biological tolerability has been confirmed repeatedly (Albrektsson, Hansson, and Ivarsson 1985; Ichikawa et al. 1992). Furthermore, several in vitro experiments have demonstrated that zirconia is capable of withstanding simulated long-term loading (Kohal et al. 2002).



Figure 1: The Tübingen Immediate Implant (Tübinger Sofortimplantat) was first developed in Germany in 1974 by Prof. W Schulte (Tübingen University) (<http://www.zahn-implantate-berlin.de/deutsch/zahnimplantat.html> 25.11.2013)

1.2 Zirconia

The development of all-ceramic zirconia is one of the most interesting chapters in dental implantology in recent years.

The German chemist Martin Heinrich Klaproth first obtained zirconia (ZrO_2) in the reaction product created by heating zircon gems in 1789. For a long time zirconia was blended with rare earth oxides and used as a pigment for ceramics (Piconi and Maccauro 1999). The first paper concerning the biomedical application of zirconia was published in 1969 (Helmer 1969). Currently, the main use of zirconia is as a ceramic biomaterial in the manufacture of ball heads for total hip replacements. This use was introduced by Christel and Meunier (1988).

Zirconia is also being used successfully in many areas of dentistry (Helmer 1969). Yttrium tetragonal zirconia polycrystal (Y-TZP) based systems are the most recent high-strength all-ceramic systems used for crowns, fixed partial dentures, endodontic posts, and implant abutments. Zirconia is also used with the CAD/CAM systems, which are in demand for both aesthetic zones and stress-bearing regions (Koutayas and Kern 1999; Boudrias et al. 2001; Brodbeck 2003; Sun et al. 2006).



Figure 2: A titanium implant and a metal-free zirconia implant. Due to the zirconia implant's appearance (white), it can now be used in highly aesthetic zones without worrying about a darker gum appearance as occurs with traditional implants (<http://www.maxillofacialcostarica.com/zirconia-implants> 25.11.2013)

Currently, zirconia is used not only because of its excellent biomechanical properties, but also its white color, which is similar to the natural coloring of teeth (Fig. 2) and permits the production of aesthetically high-quality reconstructions (Sturzenegger et al.2000).

1.3 Physical properties of zirconia

As a metal substitute, zirconia possesses good physical properties, including high flexural strength (900 to 1,200 MPa), hardness (1,200 HV 0.1), Weibull modulus (10 to 12), fracture toughness (8 MPa \sqrt{m}), and low potential for corrosion (Geis-Gerstorfer and Fäßler 1999). Zirconia is usually available as a 3-5 M% Y-TZP (Kelly and Denry 2008). Table (1) provides the mechanical and physical properties of TZP.

Table 1: Properties of zirconia (Piconi and Maccauro 1999a; Pilathadka, Vahalová, and Vosáhlo 2007).

Property	TZP Material
Color	White
Chemical composition	Zirconia and yttrium oxide 3 mol% Hafnium oxide < 2% Aluminum oxide + silicone oxide <1% Total 100%
Density, gcm ⁻³	>6
Porosity, %	<0.1
Bending strength, MPa	900–1200
Compression strength, MPa	2000
Fracture toughness, K_{1c} [MPa \sqrt{m}]	7–10
Coefficient of thermal expansion, K ⁻¹	11×10
Thermal conductivity, W m ⁻¹ K ⁻¹	2
Hardness HV 0.1	1200

1.4 Form and microstructure of zirconia

Zirconia is a well-known polymorphic material that occurs in three crystallographic forms: monoclinic (M), cubic (C), and tetragonal (T). Pure zirconia is monoclinic at room temperature. This phase is stable up to 1170°C. Above this temperature it transforms into the tetragonal phase, and then at 2370°C into the cubic phase (Fig. 3) (Goff et al. 1999).

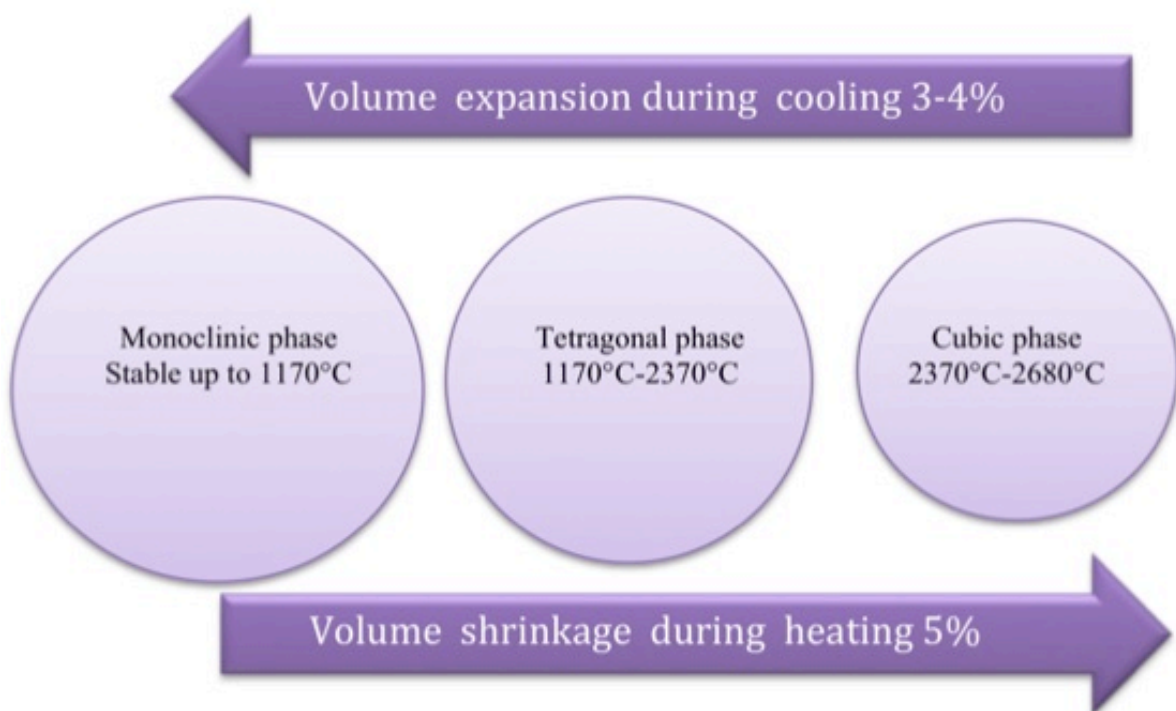


Figure 3: Zirconia phase transformation.

After sintering in the 1500—1700°C range, a T-M transformation occurs during cooling between 1070°C and 970°C. This leads to a volume expansion of approximately 3-4%, resulting in cracks in pure zirconia ceramics that break into pieces at room temperature.

In the early stages of zirconia development, Ruff and coworkers (Ruff, Ebert, and Stephan 1929) showed the feasibility of stabilizing the C-phase at room temperature by adding small amounts of CaO to the zirconia. Several solid solutions ($\text{ZrO}_2\text{-MgO}$,

ZrO₂-CaO, ZrO₂-Y₂O₃) were tested; the addition of these stabilizing oxides to pure zirconia allows the development of multiphase materials known as partially stabilized zirconia (PSZ) (Subbarao 1981). These materials were tested for biomedical applications, but research efforts in the subsequent years appeared to be more focused on zirconia-yttria ceramics characterized by fine-grained microstructures known as tetragonal zirconia polycrystals (TZP).

1.5 Surface roughness

The majority of studies on surface roughness and cell-surface interaction have been based solely on titanium surfaces. Recent implant research shows that rough surface topography is desirable for the bone integration process (Wennerberg 1996). Porous zirconia-surfaced implants with rough surfaces have been demonstrated to have better retrieval torque resistance in rabbits (Sennerby et al. 2005).

Oliva et al. (2010) studied 100 rough-surfaced zirconia implants in humans and reported a success rate comparable to that of titanium implants after 1 year. He also compared the success rates of three different roughened zirconia implant surfaces (Cera root) over a period of 5 years (coated surface, uncoated surface, and acid-etched surface). The acid-etched surface had a long-term clinical performance of 97.60% (Oliva et al. 2010).

In vitro surface roughness seems to be just as important for initial cell growth and metabolism (Payer et al. 2010). In an extensive review of the clinical effect of implant surface features, Albrektsson and Wennerberg reported significantly faster bone apposition on implant surfaces with average surface roughness (Ra) values of approximately 1.5 μm compared to surfaces with Ra values <1.0 μm (Albrektsson and Wennerberg 2004). To distinguish between different types of surface roughness, Payer et al. (2010) investigated the difference between machined smooth (ZrO₂ m) and grit-blasted surfaces (ZrO₂ g). The latter exhibits an irregular microstructure with peaks and valleys similar in dimension to grit-blasted and acid-etched titanium surfaces, whereas machined zirconia surfaces tended to be more smooth and homogeneous.

A study compared zirconia surfaces with two different titanium surfaces: machined (Ti m) and grit-blasted acid-etched titanium surfaces (Ti g+e). The profilometry results are shown in Table (2) (Gahlert et al. 2007).

Table 2: Summarized table from a study by Gahlert et al. illustrating the surface roughness of different materials.

Profilometry test	Ra, μm	Min.	Max.	SD
Ti m	0.37	0.30	0.42	0.04
ZrO ₂ m	0.39	0.28	0.52	0.09
Ti g + e	1.43	1.29	1.51	0.076
ZrO ₂ g	1.41	1.3	1.5	0.03

Zirconia implants with a roughened surface have been suggested to be capable of achieving greater stability in bone than machined zirconia implants. Roughening the turned zirconia implants enhances bone apposition and has a beneficial effect on the interfacial shear strength. Ti SLA and zirconia implants with sandblasted and machined surfaces were tested in miniature pigs. The three-dimensional roughness parameters were established as Sa, Sq, St, and Sk over a 770 μm \times 770 μm area. The removal torque of the bone implant interface was tested; at all time periods, SLA titanium implants demonstrated higher mean removal torque (RTQ) than zirconia implants (Gahlert et al. 2007).

Gahlert confirmed that the increased surface roughness of sandblasted and acid-etched zirconia implants not only has an important influence on bone integration, but is also associated with increased removal torque strength and bone stability (Table 3).

The osseointegration capacity of machined zirconia surfaces is substantially increased after modification by Al₂O₃ sandblasting. However, Gahlert confirmed that further improvements in the surface roughness of zirconia implants are needed (Gahlert et al. 2007). A very rough implant surface significantly enlarges the surface area, leading to faster osteointegration (Franchi et al. 2004).

Table 3: Topography and removal torque of the implants used in animal experimentation by Gahlert et al. (2007).

Type	Sa, μm	Sq, μm	St, μm	Sk, μm	Mean RTQ, N cm^{-1}
Ti SLA	1.15	1.44	7.55	3.71	105.2
ZrO ₂ Rough	0.56	0.72	4.55	1.74	40.5
ZrO ₂ Machined	0.13	0.17	0.96	0.38	25.9

The methods for roughening the surface of zirconia include sandblasting, acid etching, and lasering. In zirconia crowns and bridges, the creation of a highly retentive surface through nanomechanical retention between the zirconia substructure and glass ceramics can be achieved using selective infiltration etching (Aboushelib et al. 2007). However, this method has not yet been tested on zirconia implant surfaces and has not been studied at the cellular level.

Airborne particle abrasion is currently considered the most effective way to improve the surface roughness of zirconia ceramics. Nevertheless, the properties of zirconia are largely dependent on both the starting powder, which must be as pure as possible, and the fabrication technique (Aboushelib et al. 2007).

Numerous studies on implant surface roughness have shown that rough titanium implant surfaces are better than smooth surfaces due to enhanced primary stability and secondary stability (removal torque), and osteoblasts are stimulated by the rough surface both in vitro and in vivo. Now efforts are focused on making rough zirconia implant surfaces that stimulate cells and developing different methods for optimizing the surface of zirconia implants (Table 4).

Table 4: Techniques to roughen zirconia surfaces by sandblasting:

Study	Gahlert et al. 2007	Casucci 2010	Aboushelib et al. 2007	Yamashita 2009
Zirconia type	Implant Diameter: 3.75 mm Length: 10 mm	Discs Width: 1 mm Diameter: 10 mm	Discs Width: 3 mm Diameter: 11.8 mm	Discs Width: 0.5 mm Diameter: 15mm
Sandblasting material	Al ₂ O ₃ (250 µm)	Al ₂ O ₃ (125 µm)	Al ₂ O ₃ (110 µm)	SiC (125 µM)
Angle	Not mentioned	Perpendicular	Not mentioned	Perpendicular
Duration	Not mentioned	10 sec	Not mentioned	Not mentioned
Distance	Not mentioned	20 mm	Not mentioned	10 mm
Pressure	5 bar	0.41-0.68 MPa	0.35 MPa	0.4 MPa

Manufacturers of zirconia implant systems have different methods for roughening the surface, but only details about the design of the implant surface could be obtained (Table 5).

Table 5: Surface design of some commercially available zirconia implants:

Implant name	HIZ	WHITESKY	OMNIS	Z-SYSTEM	ZIT-Z
Surface design	Unstructured Etched	Microstructured Roughened	Corundum blasted Etched	Corundum blasted	Blasted

1.6 Cellular adhesion

Cell adhesion to implant surfaces is the first important step for implant success. Surface energy, charge, wettability, chemistry, and topography influence the biological response of cells and tissues to an implant (Hempel et al. 2010). Greater surface roughness ($R_a > 3.5 \mu\text{m}$) has been claimed to be the most important factor for increasing osteoblast proliferation, followed by high surface energy. The effect of wettability plays a minor role. Surface roughness is also the main factor regulating blood coagulation (Kubies et al. 2010).

The pathway of bilateral reactions after implant insertion into the host body has been reported to depend on the nature and properties of the implant surface (Okumura 2010). The physical and chemical properties of the surface trigger various cell responses that result in changes in cell adhesion to the implant (Jones et al. 1999). However, information about the influence of different zirconia surface designs on the cellular responses of osteoblasts and fibroblasts is still very limited.

In vitro studies (Kubies et al. 2011; Puleo and Nanci 1999) have described the first contact of cells with the material surface as a multi-step event. First, serum/plasma proteins adsorb on the implant surface. Next, cells attach to this protein layer and specific cell receptors, integrins, link the inside of a cell with its outside environment. This attachment regulates a wide variety of cell behaviors. Recognition of the presented extracellular ligands mediates the first interaction between cells and the material.

The adhesion process is accompanied by the re-arrangement of cytoskeleton proteins, formation of tight focal adhesion contacts, and activation of focal adhesion

kinase (FAK), which leads to the induction of several intracellular signal transduction pathways resulting in cell proliferation and differentiation (Kim et al. 2007; Puleo and Nanci 1999). In this way the surface of the material may determine the cell fate, the osseointegration of the implant, and its clinical success (Lutolf and Hubbell 2005; Hamilton and Brunette 2007).

As described in several *in vitro* and *in vivo* studies, rough biomaterial surfaces provide stronger bone fixation than smooth surfaces due to promotion of osteoblast adhesion, proliferation, and differentiation (Zvi Schwartz, Nasazky, and Boyan 2005). An experimental *in vitro* study (Hempel et al. 2010) showed that zirconia has a more pronounced effect on the adhesion, proliferation, and differentiation of human SAOS-2 cells than titanium.

An earlier study showed that a surface roughness of 1–2 μm positively affects cell proliferation (Boyan et al. 2003). The data suggested that the tested rough zirconia surfaces have the potential for osseointegration.

1.7 Aim of the study

The aim of the experiment was to develop suitable methods for roughening the zirconia surface and to study and evaluate the created surfaces in terms of their cell adhesion, proliferation and metabolic activity of human osteoblasts on zirconia surfaces of different textures and roughness compare to a titanium surface.

The following questions were addressed:

- Surface structuring:

A new method to create a rough zirconia surface by sandblasting before sintering was evaluated to optimize surface roughness. How does sandblasting before sintering enhance the surface roughness?

- Zirconia surface

Is zirconia a biocompatible material for cell adhesion, growth, and proliferation?

Does the surface roughness of zirconia influence initial cellular attachment?

- Comparison with titanium

How do different zirconia-based materials with different surface roughness behave in terms of cell adhesion, proliferation, and metabolic activity?

2. Material and methods

The favorable parameters obtained from the trial experiments were used as guidelines later in this work (Fig. 4).

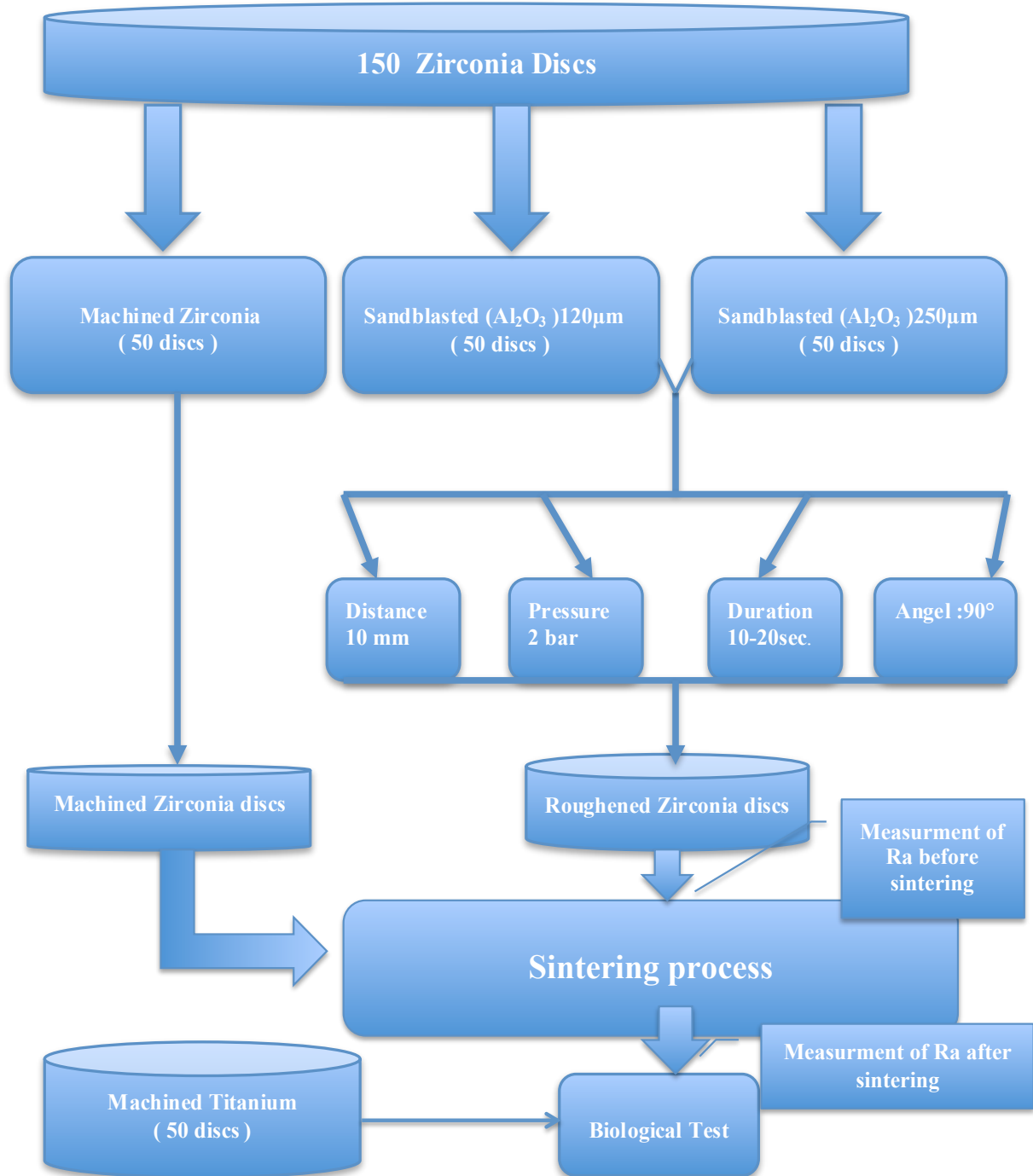


Figure 4: Study outline

2.1 Sample preparation

The objective of this experiment was to create a rough surface on tetragonal stabilized zirconia using a trademark Zenotec (Wieland DentalTechnik, Pforzheim, Germany) before the sintering procedure. Two hundred discs were divided into four groups: three groups of 50 zirconia discs and one group of 50 machined titanium discs. Two zirconia groups were roughened differently (120 μm or 250 μm Al_2O_3 sandblasting) and one group had a machined surface (Y-TZP) for comparison with the machined (grade 2) titanium group.

2.1.1 Zirconia disc preparation

A cutting machine (Accutom 50, Struers) created the zirconia discs from cylindrical bars 14 mm in diameter and 1 mm in width (Fig. 5).

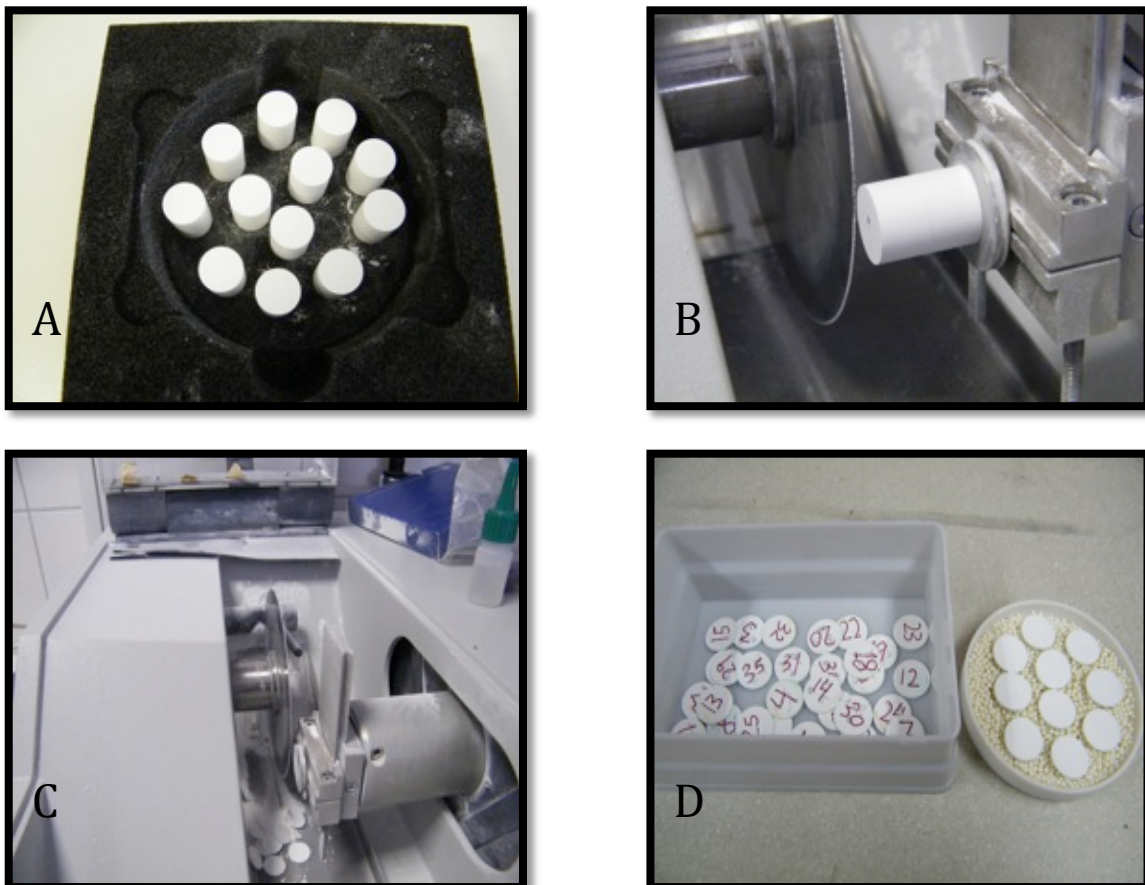


Figure 5: Production of zirconia samples using a cutting machine

The surface roughness was measured after sandblasting and the mean and standard deviation calculated for each group.

2.1.2 Titanium disc preparation

Grade 2 titanium discs 12 mm in diameter and 1 mm in width were prepared by cutting titanium plate (Goodfellow) with a punching tool. All titanium discs underwent a smoothing process using abrasive silicon carbide papers (SiC, Buehler-Wirtz, Düsseldorf, Germany) with different roughness (600, 1200, 2500, and 4000) on a grinding machine (Meta Serv, Buehler-Wirtz, Düsseldorf, Germany).

2.1.3 Sandblasting and surface roughness of zirconia samples

Before the sandblasting procedure, the surfaces of the zirconia samples were cleaned of the remnants of the powder produced by the cutting process using a strong stream of air. For easy manipulation of the zirconia discs, a special holder was made by mixing heavy silicone (Zetalabor platinum 85, Italy) inside a metal ring. One zirconia disc was centered in the middle of the silicon mold see (Fig. 6).

Sandblasting was performed with different parameters to achieve surface roughness. A specific tool was made to establish a fixed distance of 10 mm and a perpendicular angle between the sandblasting source and samples, and the duration of sandblasting was 15 sec for every disc.

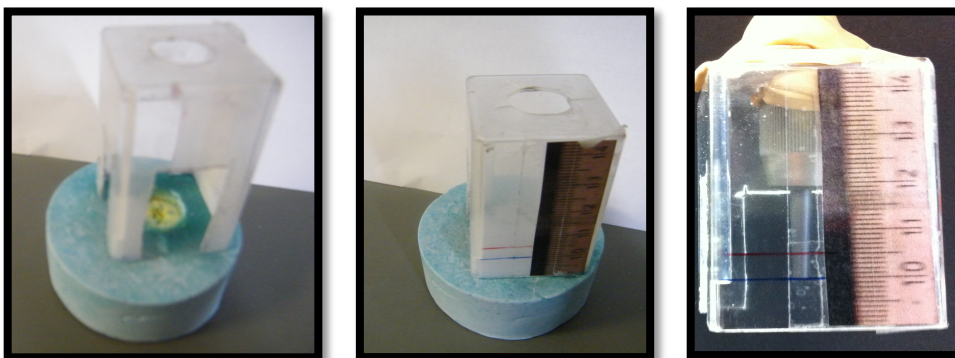


Figure 6: The tool used to control the perpendicular angle of sandblasting and constant distance of approximately 10 mm.

The sandblasting procedure in the experiment was color controlled. Occlusion spray (Omnicent, Germany) was used to paint the working surface of the samples.

Two groups of zirconia underwent the sandblasting procedure with the sandblasting machine (P-G 400, Harnisch, Rieth, Germany). The released particles pressure was 2 bar. The blasting material used for this experiment was 120 μm or 250 μm Al_2O_3 .

2.1.4 Preparing the zirconia samples for measurement of surface topography

Every zirconia sample was carefully cleaned with a strong stream of air and the residual powder was removed.

2.2 Analysis of surface topography before sintering

Zirconia discs were topographically analyzed by profilometry (Perthometer S6P, Mahr, Göttingen, Germany). Ten samples from each group were randomly tested. For surface topography, 121 profiles over a 3×3 mm area were measured. A scanning electron microscope was used (LEO1453, Zeiss, Oberkochen, Germany) for the morphological analysis. The surface structure was analyzed using a conical diamond tip with a 2 μm diameter and 90° angle (MFW-250). Surface roughness was measured in the same manner for all tested samples: Ra, Rmax, Rz, Rq, Rp, and Rt.

The average roughness, universally called Ra, is defined as the average distance between peaks and valleys of surface roughness. Ra was used in the present experiment to detect general variations in the overall profile height. The maximum roughness depth, Rmax, is the longest single roughness depth within five single roughness depths. Rz corresponds to the arithmetic average of single depths. Rq is the root mean square average of the roughness profile ordinates. Rp is the height of the highest profile peak in the roughness profile within one sampling length. Rt is the total height of the roughness profile. All of these parameters were calculated for each sample using the software for the Perthometer (version 7.0)

The Perthometer uses the mechanical profile method in which two dimensions of the object surface are recorded (DIN EN ISO 4768). A needle stylus in the form of a conical diamond tip moves perpendicularly and horizontally across the surface of the samples at a constant speed (0.5 mm/sec). The contact is constant between the tip of the needle and the surface of the sample (Fig. 7). The surface topography was

measured in 121 readings for each sample and the mean and standard deviation calculated.

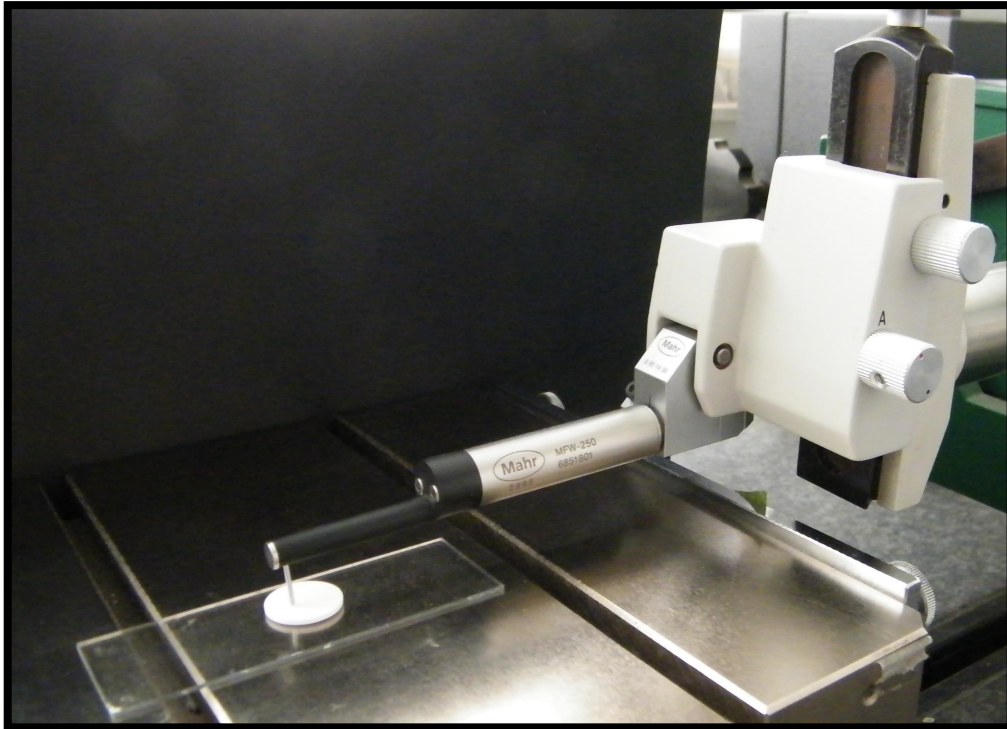


Figure 7: Perthometer used, to analysis surface roughness of samples.

2.3 Sintering process

The sintering process for zirconia discs was performed according to the manufacturer's instructions using a special furnace (Vita Zyrcomat; Vita, Bad Säckingen). See (Fig. 8). The starting temperature was the room temperature. The temperature increased over the course of 1 h to 1530°C, where it was maintained for 2 h, and then cooled to 400°C within 3 h.

After sintering the samples, the mean surface roughness and standard deviations were analyzed again for 10 random samples from each zirconia group.



Figure 8: Sintering machine for sandblasted samples

2.4 Analysis of surface topography after sintering

After the sintering procedure, surface topography was analyzed again as described above. (See section 2.2)

2.5 Cleaning the samples and preparation for biological tests

For the cell culture test, all samples were cleaned and sterilized, and all discs underwent the same cleaning and preparation procedures. Every disc was marked on the non-working surface for orientation.

Prior to cell cultivation, the discs were cleaned ultrasonically (Sonorex super RK102H) from Bandelin, Germany) at 45°C for 15 min and sterilized with 70% ethanol for 10 min followed by pure 100% alcohol for 10 min in a sterile workbench (Lamin Air HB2472). All samples were then preserved in a Petri dish and kept in the in sterile workbench until the experiments were completed.

2.6 Biological tests

Biological tests were performed to determine the effect of different zirconia surface characteristics on cell viability, adhesion, and proliferation compared to titanium discs. The biological tests consisted of three specific assays: XTT, BrdU, and crystal violet.

2.6.1 Osteoblast cell culture

The cell line used for this experiment was SAOS-2 osteoblasts (DSMZ, Germany), which originated from human osteogenic sarcoma. The cells were cultured in 75 cm² sterile cell culture flasks with canted neck (Costar, Corning, USA) under standardized conditions at a temperature of 37°C and atmosphere of 5% CO₂ in an incubator (CO₂-Auto-zero -Heraeus). The culture medium was 10 ml modified McCoy's 5A (Sigma-Aldrich Chemie GmbH, Stinheim, Germany) containing 10% fetal calf serum (FCS; PAA Lab, GmbH, Linz, Austria), 1% penicillin (10 mg/ml, Firma Gibco), and 1% 200 mM L-glutamine (PAA Labor GmbH, Linz, Austria). The culture medium was replaced with fresh medium twice a week. When cells reached confluence, they were rinsed twice with phosphate buffered saline (PBS; Gibco) for five min each.

The living cells adhered to one another and to the flask base. For harvesting, the adherent cells were separated by trypsinization with the addition of 1.5 ml trypsin-EDTA (0.05% trypsin/0.02% EDTA; Gibco) for 5 min at 37°C in the incubator. Five milliliters of fresh modified McCoy's 5A medium was added to stop digestion and 10 µl from the new culture taken up by volumetric pipette to count the number of cells using a hemocytometer (C-chip, Digital Bio, Korea) and cell suspension slide under the microscope (Olympus CK2).

The number of cells in the corner squares was divided by 4 to calculate the average number of cells per square and multiplied by a factor of 1×10^4 to calculate the number of cells per milliliter. The concentrated cell suspension was diluted with medium to the respective seeding concentration for cell culture tests.

2.6.2 Crystal violet test of adhesion and cell coverage

The adherent osteoblasts on the disc surface were stained with violet pigment and the color measured using an ELISA reader to clearly see the effect of different surface topography on cell adhesion. Under the microscope, cells spread over and adhering to the different zirconia surfaces were visible because of the high contrast between the violet-colored cells and the zirconia discs.

2.6.3 Crystal violet test of initial adhesion

For the adhesion test, the cell density for inoculation was approximately 1×10^5 cells/cm² and the well surface was 1.8 cm² for a 24-well culture plate (Cluster, Corning USA). Therefore, 1.8×10^5 cells were required for each well and seeded in 1000 μ l modified McCoy's 5A medium. The cultivation time was adjusted to 1 hour as this time proved sufficient in pre-test experiments of adhesion.

After the discs were cleaned and sterilized, they were transferred to 24-well culture plates under sterile conditions. For each surface, there were four samples and four background controls, resulting in 32 samples being examined for each experiment.

The number of cells required for each experiment was 2.88×10^6 cells for 16 samples. The discs were centered in the middle of the microtiter plate and the cell suspensions seeded on the middle of the samples. After one hour under standardized conditions at 37°C in an atmosphere of 5% CO₂, the microtiter plate was removed from the incubator (CO₂-Auto-zero-Heraeus).

In a sterile workbench, the medium from the cell culture plate was carefully removed using jet pump suction and the samples repositioned in a new microtiter plate. Because so many cells were attached to the sidewall and base of the samples, which will result in inaccurate readings later, the test samples were transferred to a new cell culture plate and washed with 800 μ l Hank's washing solution. The next step was fixation; the adherent cells were affixed to the zirconia discs using 800 μ l of 3% paraformaldehyde in PBS for 15 min at room temperature. The fixation solution was then subsequently removed by jet pump suction.

The cells were stained with 500 μl 0.5% crystal violet (Sigma) in 20% methanol solution (Merck) for 15 min at room temperature. Next, the discs were rinsed with 500 μl PBS at least 3 times each. The discs were moved to another cell culture well to determine the color of the adherent cells only. The last step of this test was to measure the color density, which represents the number of cells attached to each sample. Methanol (500 μl) was added and the samples carefully agitated for 5 min to extract the violet color, which was measured with an ELISA reader (Fig. 9).

2.6.4 Crystal violet test of cell coverage

For the cell coverage and spreading test, the cell density for inoculation was approximately 3×10^4 cells/cm² and the well surface was 1.8 cm² for a 24-well culture plate (Cluster, Corning USA). Therefore, $1.8 (3 \times 10^4)$ cells were required for each well and seeded in 1000 μl modified McCoy's 5A medium. The cultivation time was adjusted to 72 hour as this time proved sufficient in pre-test experiments. The next steps of this experiment have been already discussed in details (See section 2.6.3). Test of cell coverage and spreading is shown in (Fig. 9) determined by staining SAOS-2 osteoblast with crystal violet after 72h.

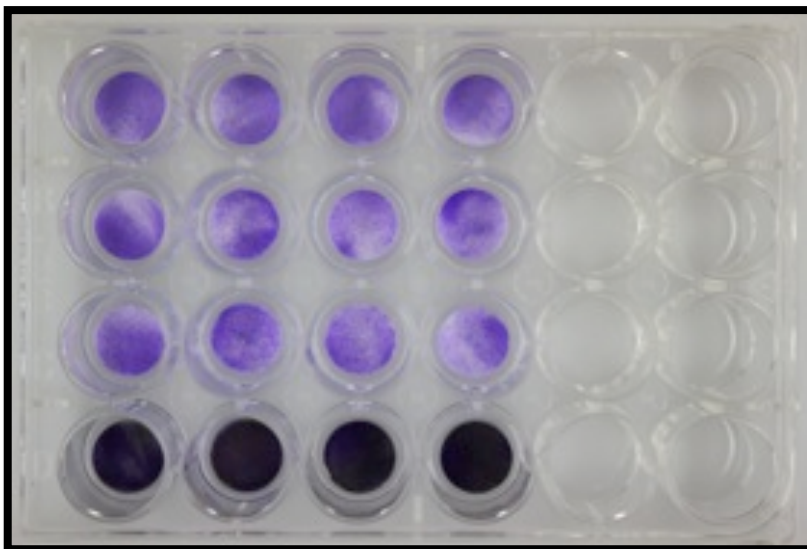


Figure 9: Example of a crystal violet test in which the samples exhibit different concentrations of color depending on the number of cells in each sample. This step is after washing with Hank's solution and before the elution of the colored cells. The dark samples in the bottom row are the titanium discs.

2.6.5 Test of metabolic activity and proliferation

To investigate the metabolic activity and proliferation of osteoblasts on zircon dioxide, two standard laboratory techniques were used. Metabolic activity was assayed by the XTT test and cell growth quantified by the BrdU (5-bromo-2-deoxyuridine) assay, also known as the proliferation test. In each test, a reference substance (polished zirconia) was used as a control group.

2.6.5.1 Principle of the XTT assay

The XTT cell proliferation assay was first described in 1988 (Scudiero et al. 1988) as an effective method for measuring cell growth and drug sensitivity in tumor cell lines. XTT is a colorless or slightly yellow compound that becomes bright orange when reduced.

The XTT test, also called the cell viability assay, is a colorimetric assay for analyzing the number of viable cells based on the cleavage of tetrazolium salts added to the culture medium. This technique requires neither washing nor cell harvesting, and the complete assay from the onset of the microculture to data analysis by an ELISA reader is performed in the same microplate. Thus, the XTT test measures the metabolic activity of mitochondria in SAOS-2 osteoblast cells based on the principle of the formation of a dye by mitochondrial dehydrogenase. The quantity of dye formed within a determined time will be measured with a photometric ELISA reader. The XTT test was performed using XTT-Cell Proliferation Kit 2 (Boehringer Mannheim), which consists of XTT labeling reagent and an electron-coupling reagent.

2.6.5.2 Principle of the BrdU proliferation test

The BrdU cell proliferation assay detects 5-bromo-2'-deoxyuridine (BrdU) incorporated in cellular DNA during cell proliferation using an anti-BrdU antibody. When cells are cultured with labeling medium containing BrdU, this pyrimidine analog is incorporated into the newly synthesized DNA of proliferating cells in place of thymidine. After removing the labeling medium, cells are fixed and the DNA denatured with fixing/denaturing solution. The anti-BrdU mouse mAb is added to detect the incorporated BrdU. Denaturing is necessary to improve the accessibility of

the incorporated BrdU to the detection antibody. Anti-mouse IgG horseradish peroxidase (HRP)-linked antibody is then used to recognize the bound detection antibody.

HRP catalyzes the conversion of the fluorogenic substrate to a blue coloured product. The magnitude of the absorbance is proportional to the quantity of BrdU incorporated into cells, which is a direct indication of cell proliferation.

2.6.5.3 XTT and BrdU procedures

Both the XTT assay and BrdU test were carried out on the same samples. Zirconia samples were compared with the titanium samples and polished zirconia was used as a reference surface.

Metabolic activity was measured with the XTT assay after 48 h and proliferation by the BrdU assay during the 24-48 h labeling period SAOS-2 osteoblasts were used for these tests. The cell suspension was made as described above. The incubation period for the cell culture was 48 hours.

The samples were cleaned and sterilized, and then distributed into 24 well microtiter plates under sterile conditions. Four samples were tested with cells and four samples were treated as background controls (without cells) for each group. All samples were centered in the middle of the wells of the microtiter plate.

The number of cells seeded was approximately 3×10^4 cells/cm² suspended in 1000 μ l modified McCoy's 5A medium per well. The cells were incubated for 24 h. Next, 100 μ l BrdU labeling solution was added to each well and incubated at 37°C in the 5% CO₂ incubator.

After 44 h the microtiter plate was taken from the incubator and the samples transferred to a new microtiter plate for the XTT test. The assay was started by adding a mixture with a ratio of 2.5 ml Reagent 1 to 50 μ l Reagent 2.

The XTT labeling mixture was added (500 μ l) and incubated at 37°C in the 5% CO₂ incubator for 2-4 h until the orange color developed.

The developed color was measured in a 96-well microtiter plate containing 250 μ l of the colored solution using the ELISA reader (340 ATTC SLT Lab instruments GmbH) with a wavelength of 492/620 nm.

The proliferation test (BrdU–incorporation test) was evaluated on the same samples after termination of the XTT test. As described earlier, 100 μ l BrdU labeling solution had been added to each well 24h after the beginning of the experiment. Twenty-four hours after adding the BrdU labeling solution, FixDenat (800 μ l/well) was added and incubated for 30 min at room temperature (15°- 25°C) for cell fixation. The FixDenat solution was then removed by jet pump suction.

Anti-BrdU was prepared in this proportion: 5 ml (antibody dilution) + 50 μ l (antiBrdU). An amount of 300 μ l was added to each well and incubated for approximately 90 min at room temperature (15°C - 25°C) or in the incubator for 60 min.

Anti-BrdU was absorbed by jet pump suction, and the antibody conjugate was removed by flicking and rinsing the wells three times with 400 μ l PBS per well. The washing solution was gently tapped and removed by jet pump suction. The substrate was added (500 μ l/well) and incubated for 10 min at room temperature until the color development was sufficient for photometric detection. Stop solution was added (62.5 μ l 1M H₂SO₄) to each well and mixed by tapping gently.

Measurements were carried out within 5 min of adding the stop solution. Samples (250 μ l) were removed from each well of the 24-well microtiter plate by pipetting into a 96-well microtiter plate and measured with an ELISA reader at a wavelength of 492/620 nm.

2.7 Data analysis

2.7.1 Data analysis of surface topography and roughness

Roughness was measured for four samples per surface type (121 single profiles per sample). Using the software Perthometer, the surface characteristics and values were visualized as graphical figures with a color scale.

Fifty samples were used for each group, resulting in a total of 200 samples (150 zirconia discs and 50 titanium discs). Ten samples were randomly chosen and tested from each zirconia group. The roughness values for each surface were analyzed independently, and the mean surface roughness and standard deviation calculated before and after the sintering process.

2.7.2 Data analysis for cell adhesion and cell spreading

All surfaces were investigated three times in independent experiments, and four parallel samples were used per test group and control group, requiring a total of 32 discs per test. The ELISA reader was used and the mean and standard deviation calculated after subtraction of the means calculated for the background controls in each respective group to compare the result of repeated experiments, the machined (m) zirconia surface was used as internal reference. For each experiment, the respective means for this surface was set to 100%, and all data from other surfaces were related to this reference. This allowed plotting of the combined means of three experiments.

2.7.3 Data analysis of metabolic activity (XTT) and proliferation (BrdU)

In these experiments, the same samples were used for both the XTT and BrdU tests. The required number of samples was four per group plus four controls. The XTT assay was performed first and then the BrdU incorporation determined with the ELISA reader. The mean and standard deviations were calculated.

3. Results

3.1 Surface roughness and topography

Surface roughness and topography were analyzed using a Perthometer. The working surfaces of the samples were recorded according to DIN standards (See section 2.2 and Fig. 13-17).

3.1.1 Surface roughness

Surface roughness was evaluated in 121 single profiles per sample. Ten samples were randomly chosen and tested from each group. The mean R_a , R_{max} , R_z , R_q , R_p , and R_t and standard deviations were calculated.

An obvious difference in roughness was noted among sandblasted and machined zirconia surfaces (Table 6). However, the difference between the sandblasted samples were minimal; the samples sandblasted with 250 μm Al_2O_3 exhibited a little more surface roughness than the samples sandblasted with 120 μm Al_2O_3 under the same conditions.

The maximum roughness was attainable before the sintering process after sandblasting the samples with 250 μm Al_2O_3 ($R_a = 4.01 \mu\text{m}$ vs. after sintering $R_a = 3.86 \mu\text{m}$), but the difference in surface roughness before and after sintering was minimal (0.15 μm).

The R_a value was less for the group sandblasted with 120 μm Al_2O_3 (before sintering $R_a = 3.17 \mu\text{m}$, after sintering $R_a = 2.95 \mu\text{m}$), and the difference in surface roughness before and after sintering was also minimal (0.22 μm).

For the machined and polished zirconia group that was only sintered, the difference in the R_a value before and after sintering was negligible (0.04 μm ; before sintering $R_a = 0.31 \mu\text{m}$ vs. after sintering $R_a = 0.27 \mu\text{m}$). For the machined titanium samples the surface roughness was also measured ($R_a = 0.16 \pm 0.01 \mu\text{m}$).

Table 6: Surface roughness analysis of zirconia samples, shows very rough surfaces in sandblasted samples after sintering.

Zirconia Samples	$R_a, \mu\text{m}$	$R_{\text{max}}, \mu\text{m}$	$R_z, \mu\text{m}$	$R_q, \mu\text{m}$	$R_p, \mu\text{m}$	$R_t, \mu\text{m}$
Machined	0.27	2.61	1.97	0.35	1.05	2.74
Sandblasted with 120 μm Al_2O_3	2.95	20.60	16.77	3.70	7.78	21.54
Sandblasted with 250 μm Al_2O_3	3.86	26.95	21.11	4.85	9.99	28.17

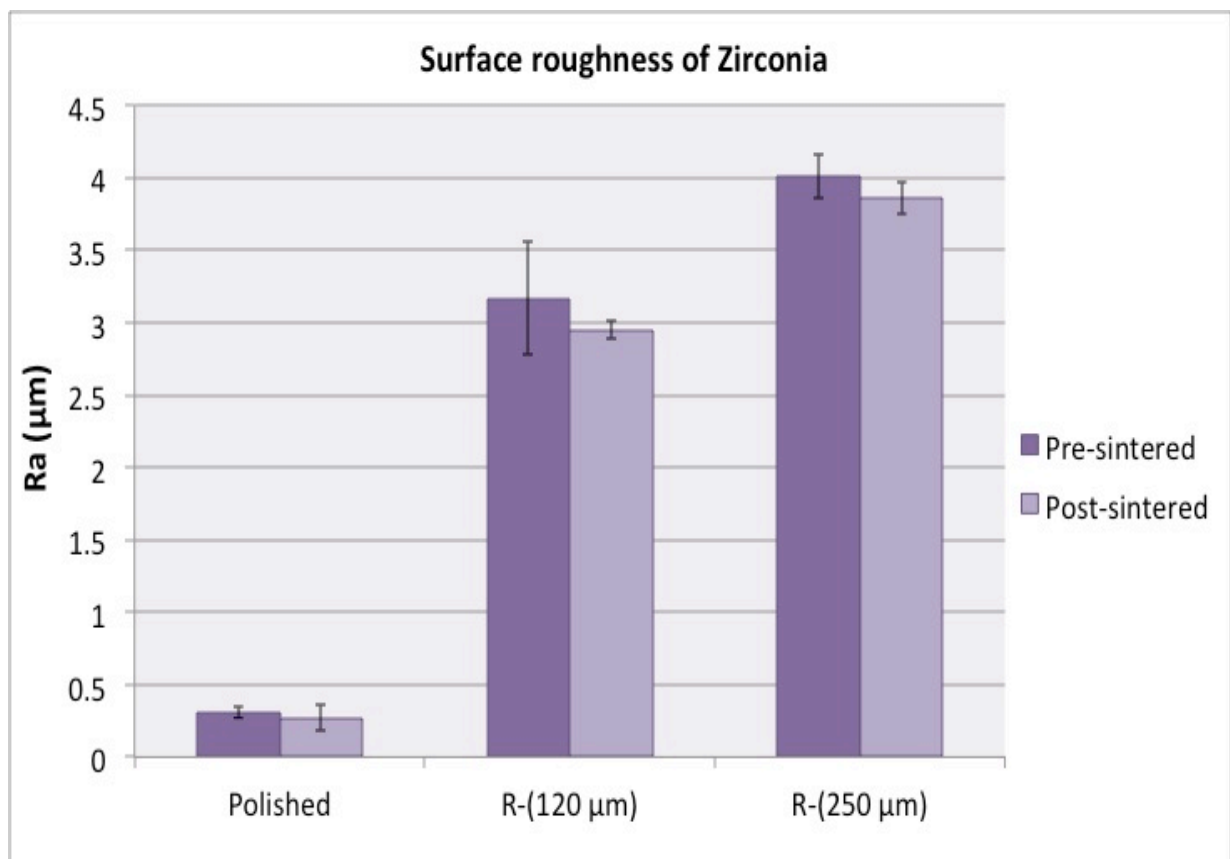


Figure 10: Average surface roughness of zirconia samples \pm SD. Note that the sandblasting before sintering provides an easy way to obtain a rougher surface.

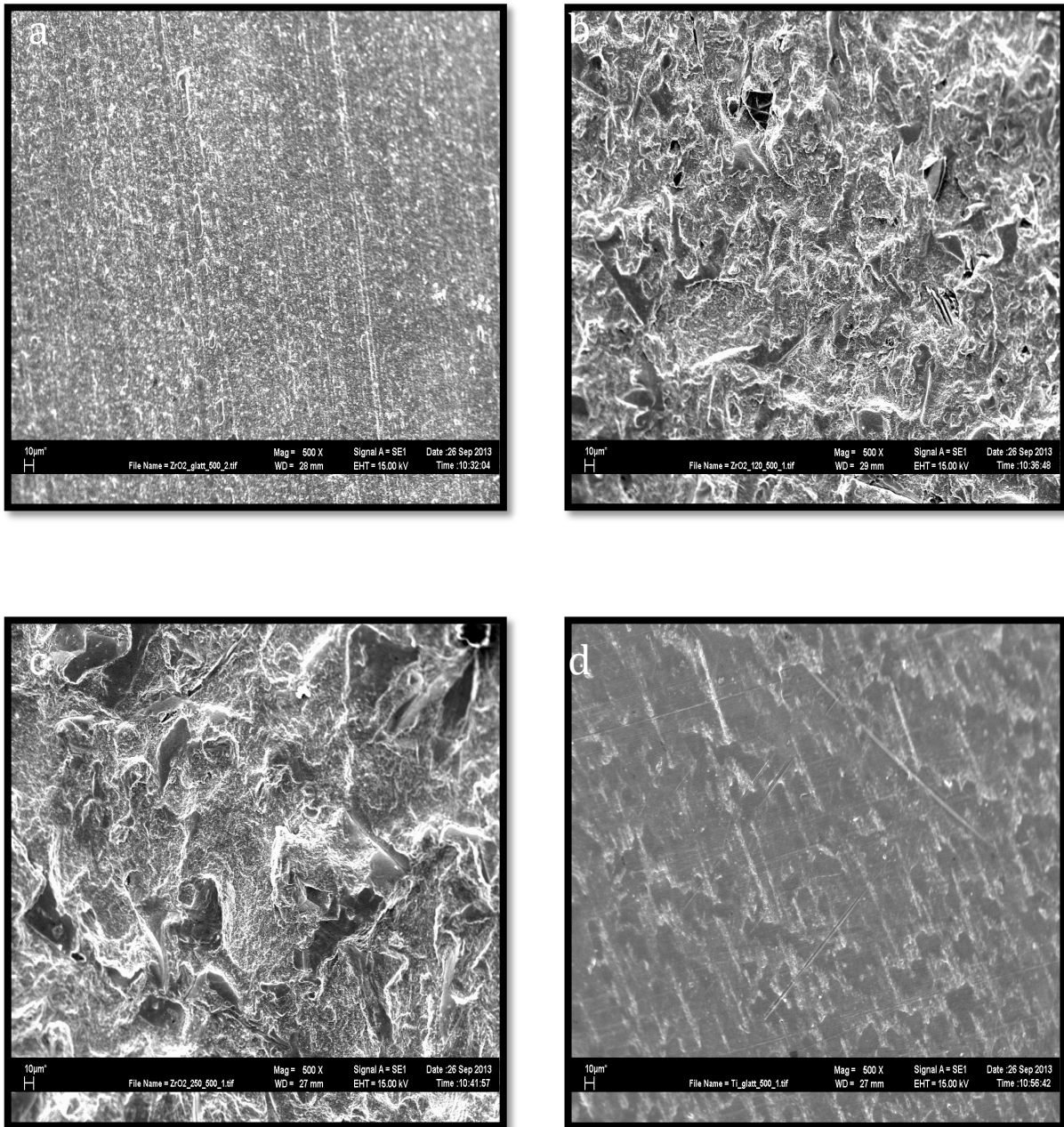


Figure 11: Scanning electron microscopy of different sintered zirconia samples and titanium. a) machined zirconia, b) rough zirconia sandblasted with 120 µm Al₂O₃, and c) rough zirconia sandblasted with 250 µm Al₂O₃ d) machined titanium sample.

3.1.2 Topography

The tested samples had different graphical representations of the smooth, sandblasted with 250 µm, and sandblasted 120 µm. One of the interesting aims of this study was to determine how the roughness is affected by sandblasting before and after the sintering process, which show clearly that sandblasting before sintering

can create a very rough surface, which is minimally reduced after subsequent sintering process due to shrinkage of the material (Fig. 10,11&12). However, the surface roughness of the machined zirconia and titanium were also investigated as machined zirconia was the reference material and titanium used for comparison. (Fig.17).

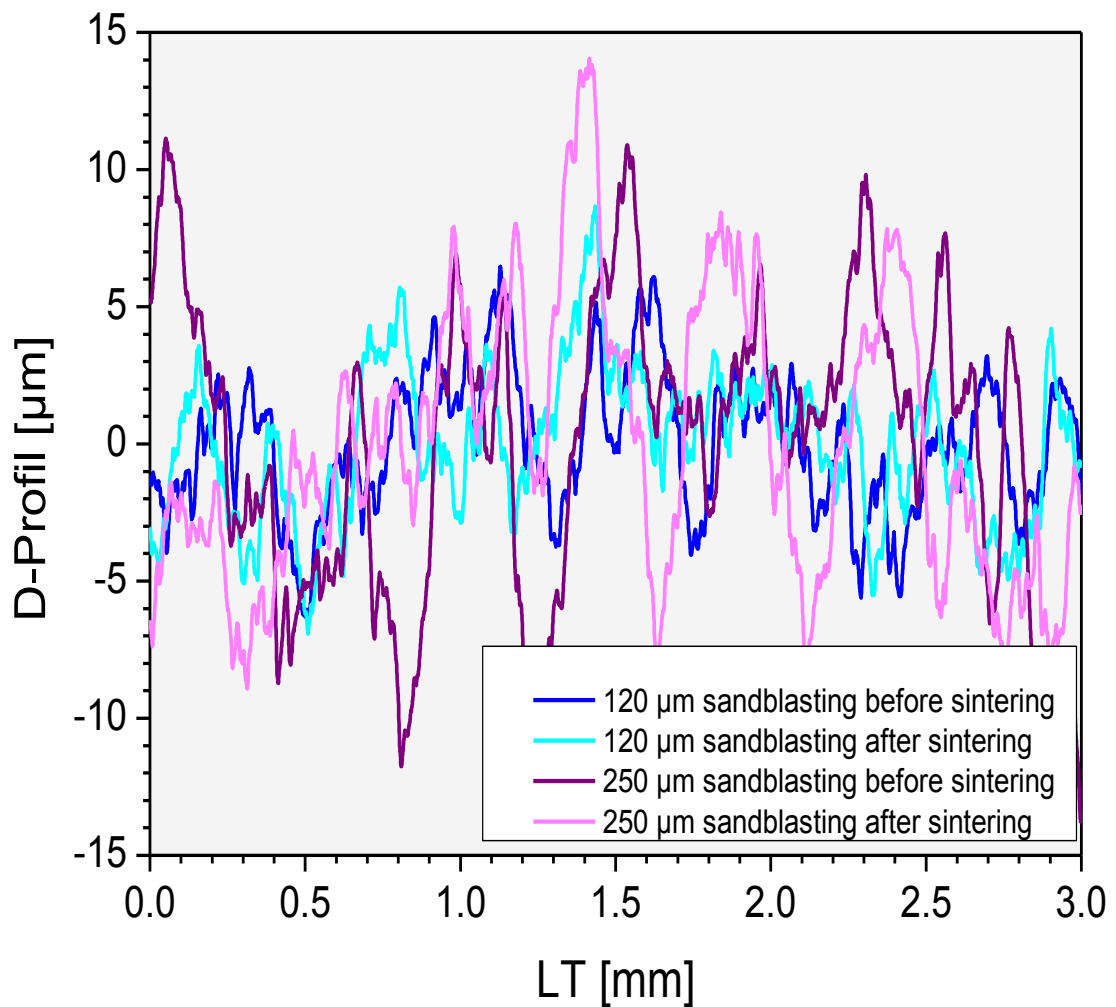


Figure 12: D-Profile of sandblasted zirconia samples before and after sintering (mean curves of 10 samples).

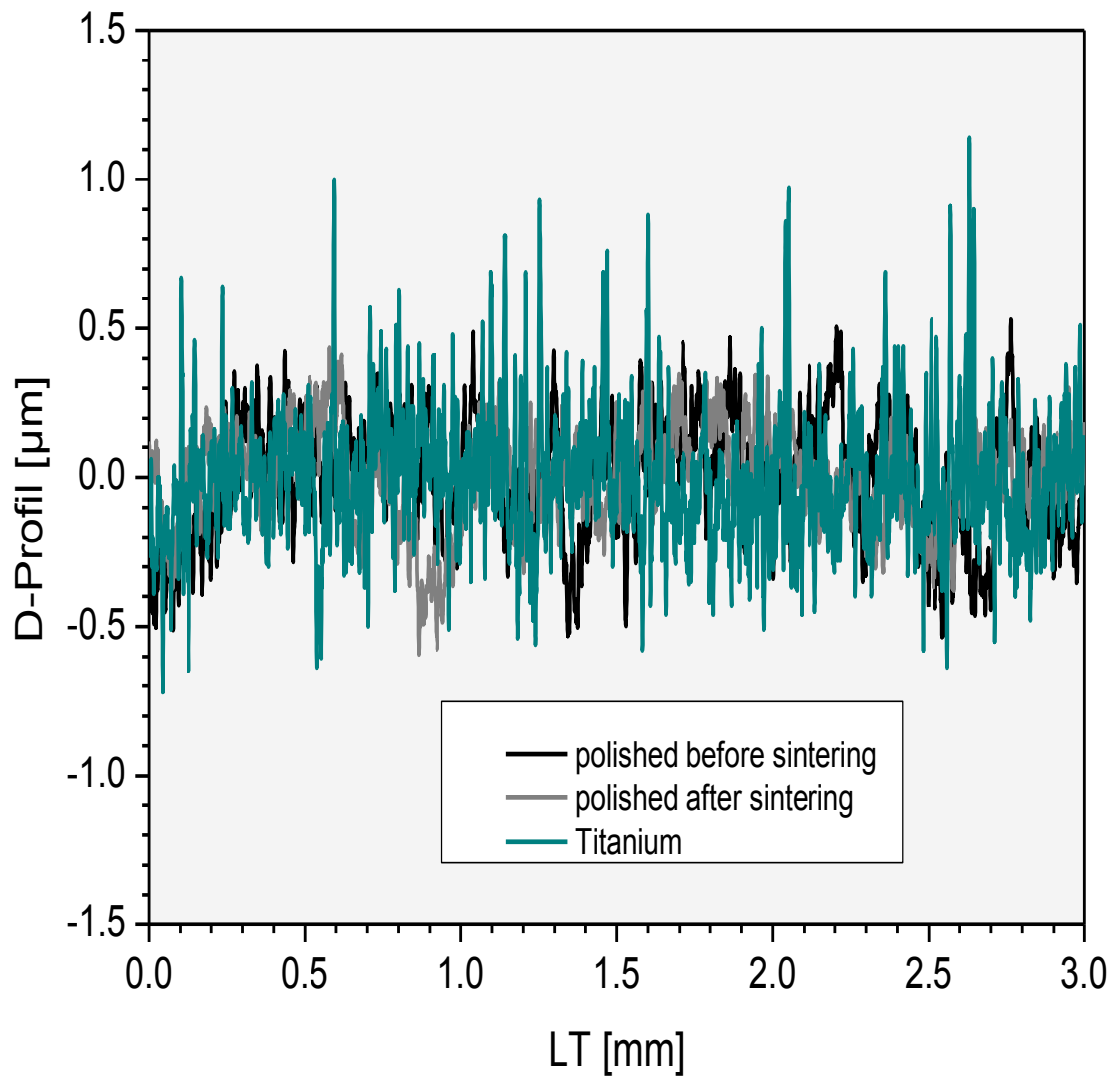


Figure 13: D-Profile of 10 machined zirconia samples before and after sintering using titanium as a reference material.

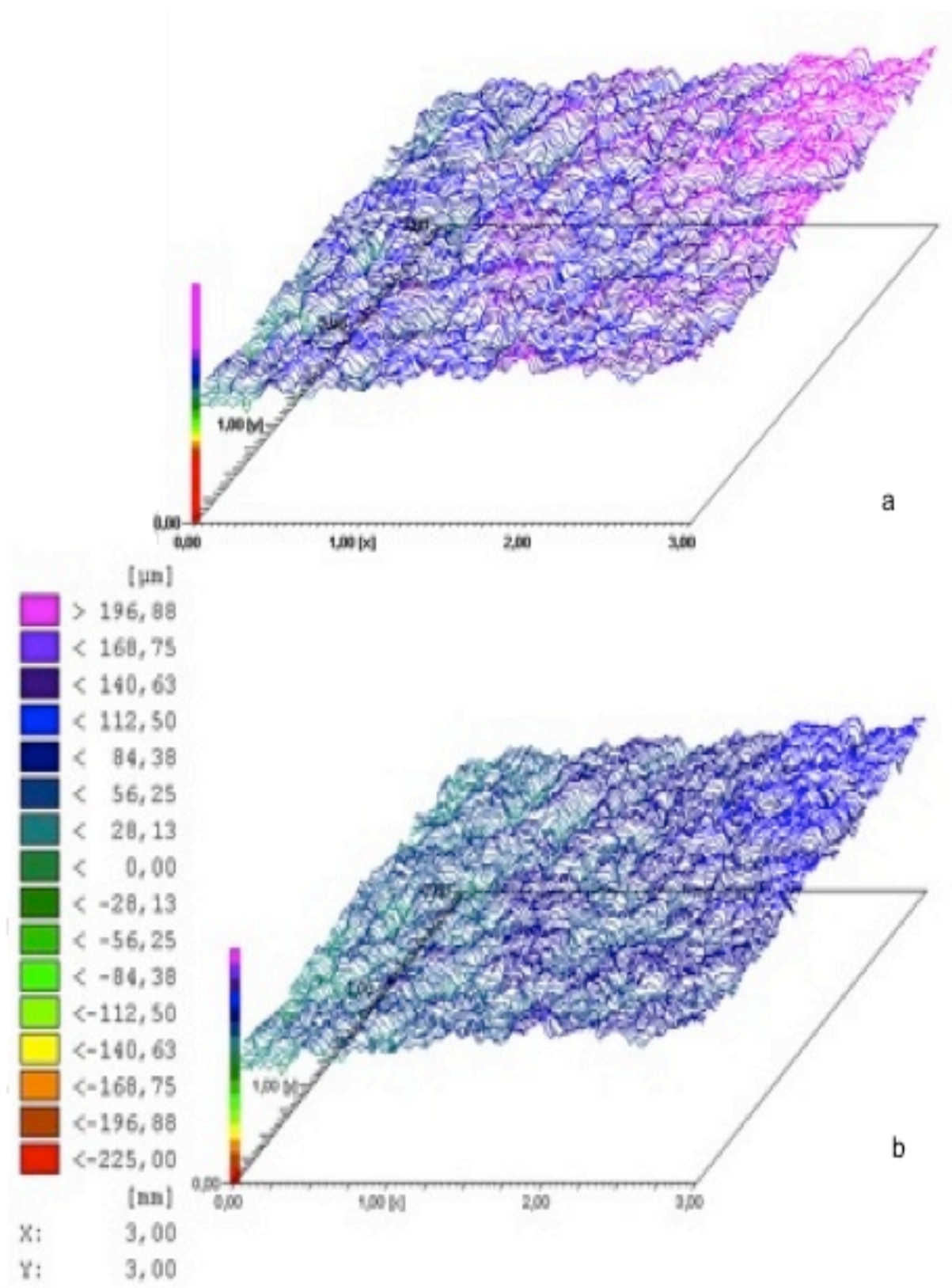


Figure 14: Surface roughness of a) a zirconia disc sandblasted with 250 μm Al₂O₃ before and b) after the sintering process. The topography is represented by the color scale.

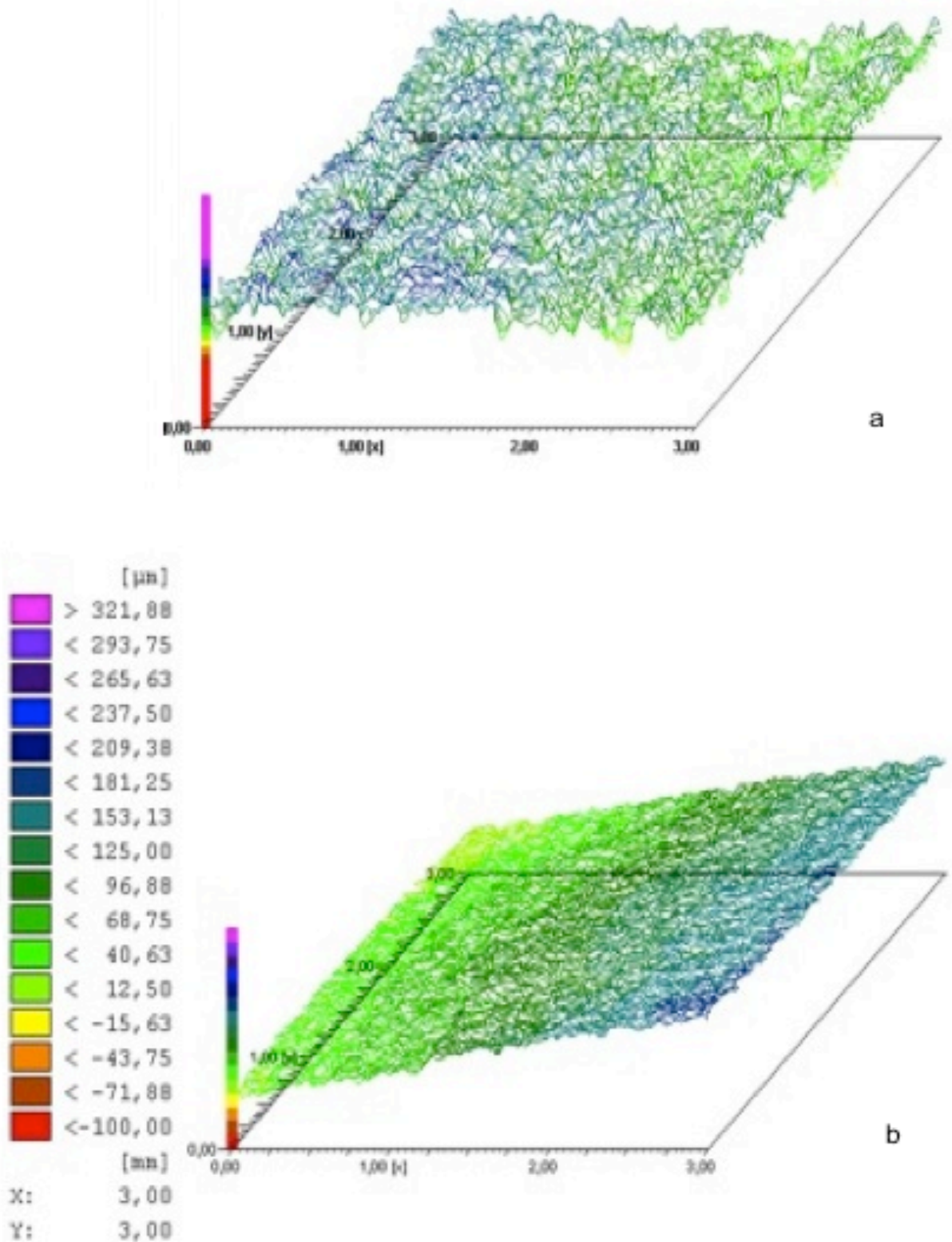


Figure 15: Surface roughness of a) a zirconia disc sandblasted with 120 μm Al₂O₃ before and b) after the sintering process. The topography is represented by the color scale.

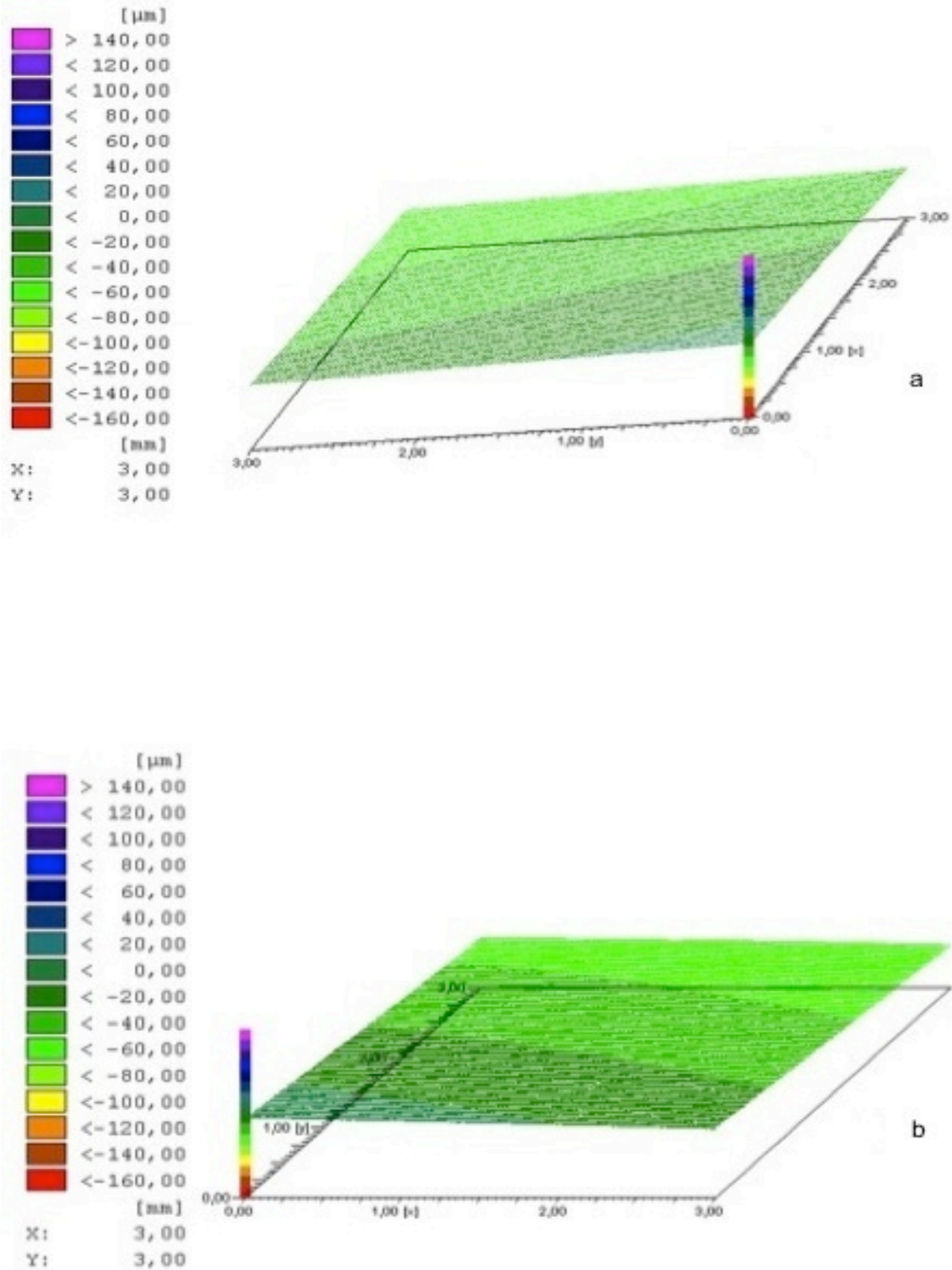


Figure 16: Surface roughness of a) a machined zirconia disc before and b) after the sintering process. The topography is represented by the color scale.

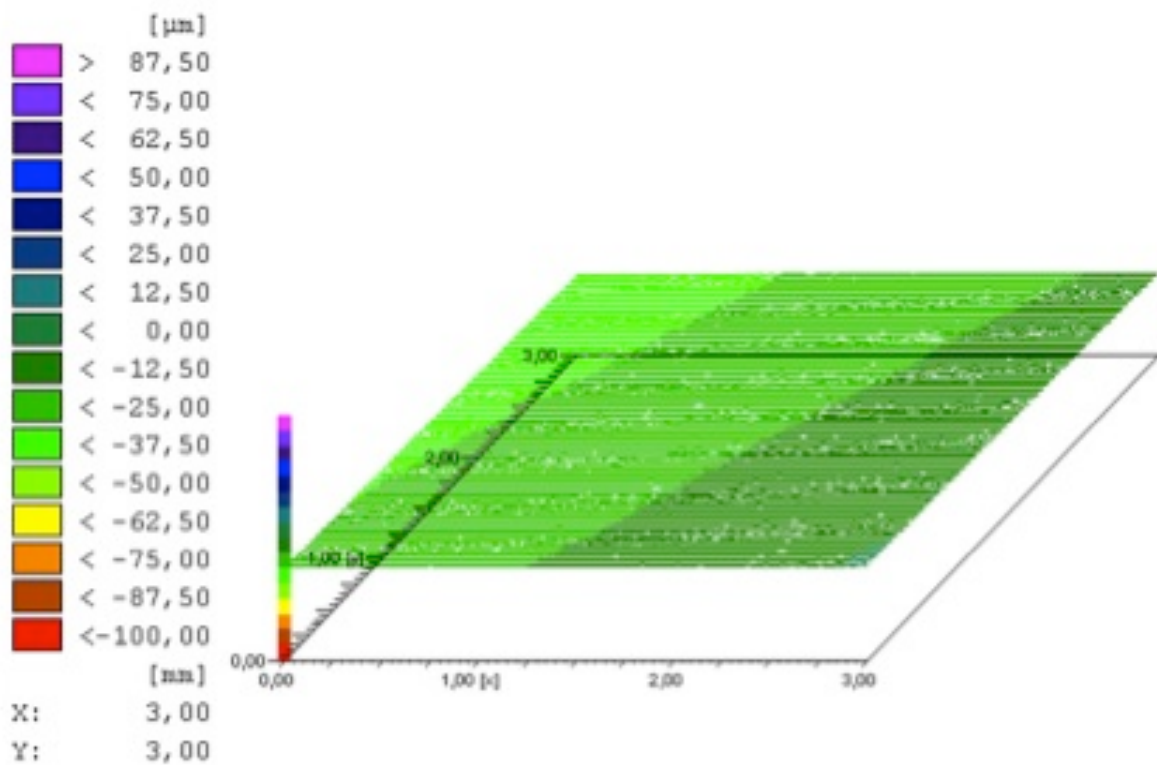


Figure 17: Surface roughness of a smooth titanium samples. The topography is represented by the color scale.

3.2 Adhesion and cell coverage

In the cell adhesion test with SAOS-2 osteoblasts, different behaviors were observed in response to the surface texture and sample material. The favorable surface for cell adhesion was the roughest surface; zirconia sandblasted with (250µm Al₂O₃), whereas the least favorable surfaces were the machined zirconia and machined titanium. Fig. (18) is a graphical representation of one test from three tests, and the results of all three tests are summarized in (Fig.19).

3.2.1 Adhesion test

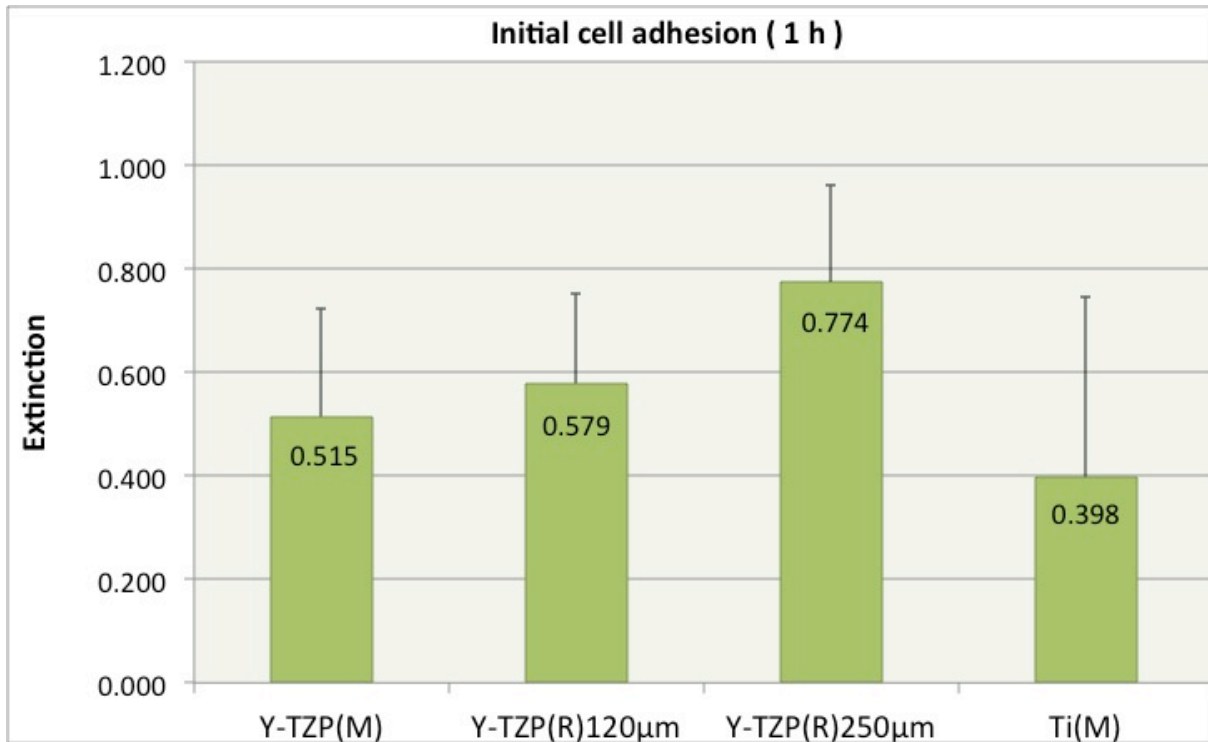


Figure 18: Initial cell adhesion of SAOS-2 osteoblasts after 1 h. A typical experiment is shown. Bars represent means and S.D. from four samples in each group. Initial cell adhesion was determined by staining with crystal violet and measuring the eluate of stained cells with an ELISA reader (wave length 550 nm).

As shown in Fig. (18), the rough zirconia surfaces positively enhanced the initial cell adhesion of osteoblast cells. The samples sandblasted with 250 µm Al_2O_3 represent a high affinity, but there was no significant difference between the two sandblasted zirconia groups (0.774 vs. 0.579; Fig. 18). For the machined surfaces, the adhesion was less and the difference was minimal (0.515 for machined zirconia vs. 0.398 for machined titanium), but the standard deviation of machined titanium was higher.

The combined data from three experiments (Fig. 19) confirmed that the percentage of osteoblast cell adhesion was generally higher on the rough surfaces of samples sandblasted with Al_2O_3 . Little difference was measured between the machined surfaces of zirconia and titanium, and both had less potential to positively enhance the osteoblast cells.

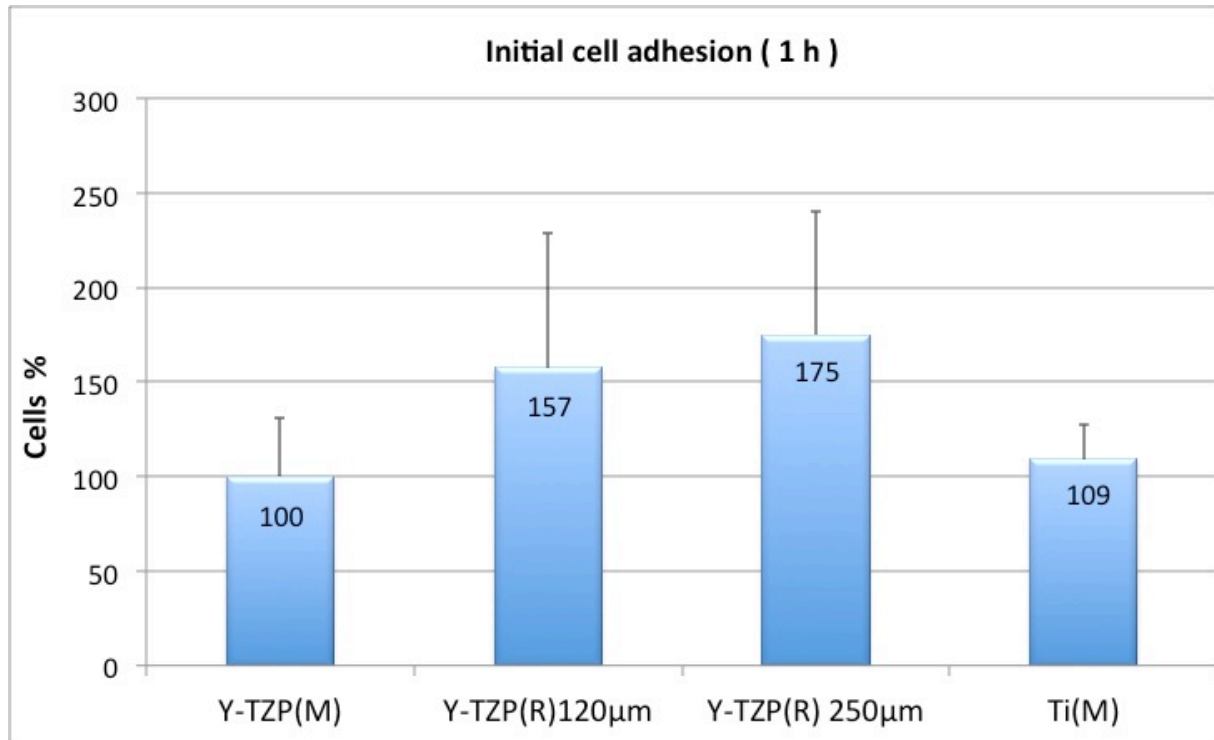


Figure 19: The means of three experiments of Initial cell adhesion after 1 h. determined by crystal violet staining are shown with standard deviations. Four samples were tested per group in each experiment (total n=12). Machined zirconia was used as a reference and set to 100%. The number of initially adhered cells was greater on the rough zirconia surfaces.

The machined zirconia was a reference specimen and set to 100%. The percentage of cells adhered to the machined titanium was 109% while in the roughened zirconia surfaces the percentage of adhered cells to the samples sandblasted with (120 µm Al_2O_3) was (157%) and the samples sandblasted with (250 µm Al_2O_3) was the highest value (175%).

SEM was also used to observe the initial adhesion of osteoblast cells on tested samples (Fig. 20 a-h).

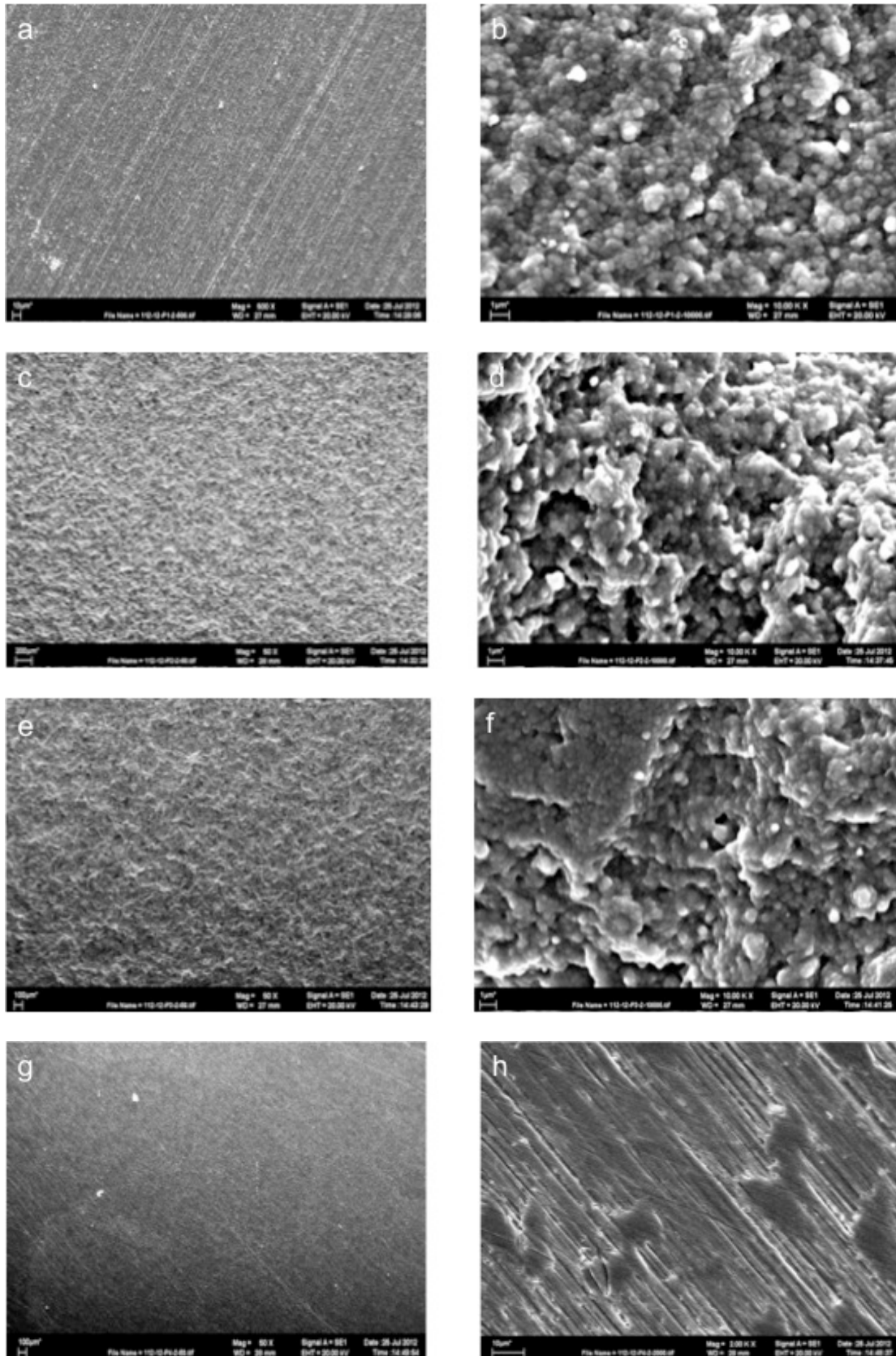


Figure 20: SEM of initial adhesion of osteoblast on various surfaces. A, b) smooth zirconia; c, d) zirconia roughened with 120 μm Al₂O₃; e, f) zirconia roughened with 120 μm Al₂O₃; g, h) smooth titanium.

3.2.2 Cell spreading and surface coverage

Surface coverage of the samples was determined by staining SAOS-2 osteoblast with crystal violet after 72h. (Fig. 21) is graphical representation of one typical test from three tests, and the results of all three tests are summarized in (Fig. 22).

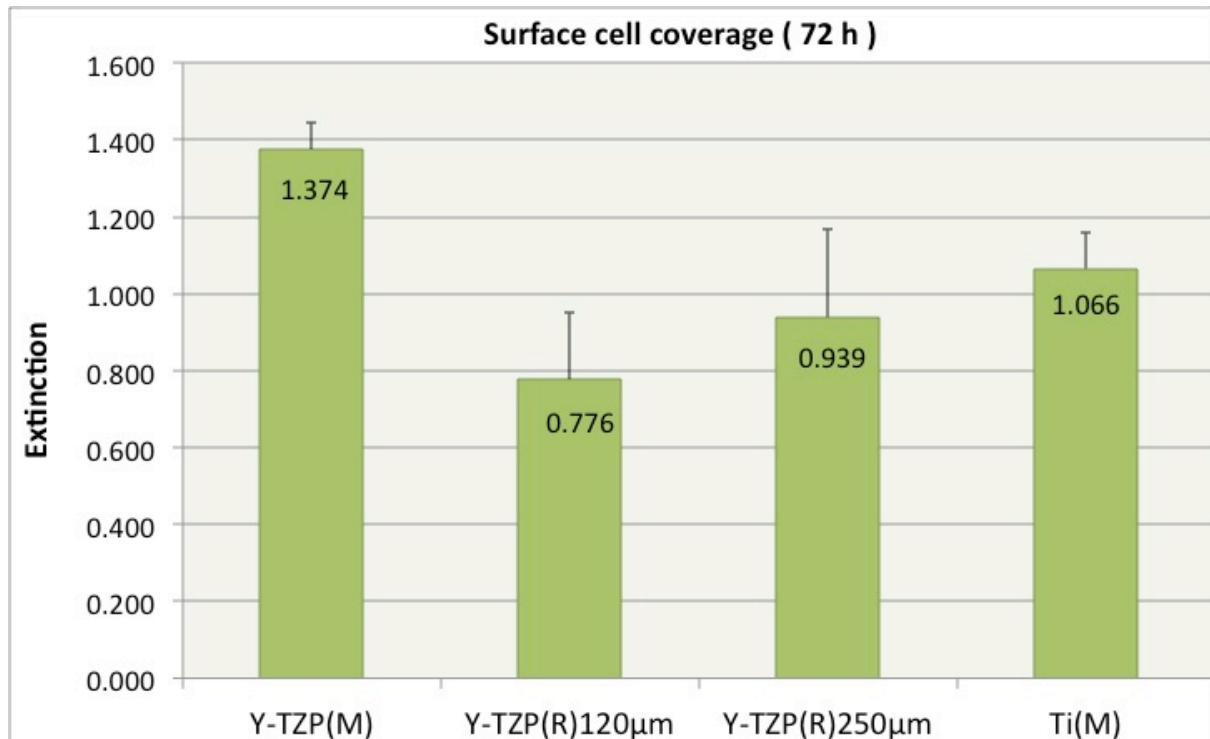


Figure 21: Surface coverage of SAOS-2 osteoblast cells after 72 h. A typical experiment is shown Bars represent means and S.D from four samples in each group. Cell coverage was determined by staining with crystal violet and measuring the elution of stained cells with an ELISA reader (wave length 550 nm).

As shown in (Fig. 21,22), osteoblast cells favored the machined surfaces of zirconia and titanium. The extinction value was (1.374 for the machined zirconia vs. 1.066 for the machined titanium). In roughened surfaces, the extinction value was less (0.776 for the samples sandblasted with 120 µm Al₂O₃ vs. 0.939 for the samples sandblasted with 250 µm Al₂O₃).

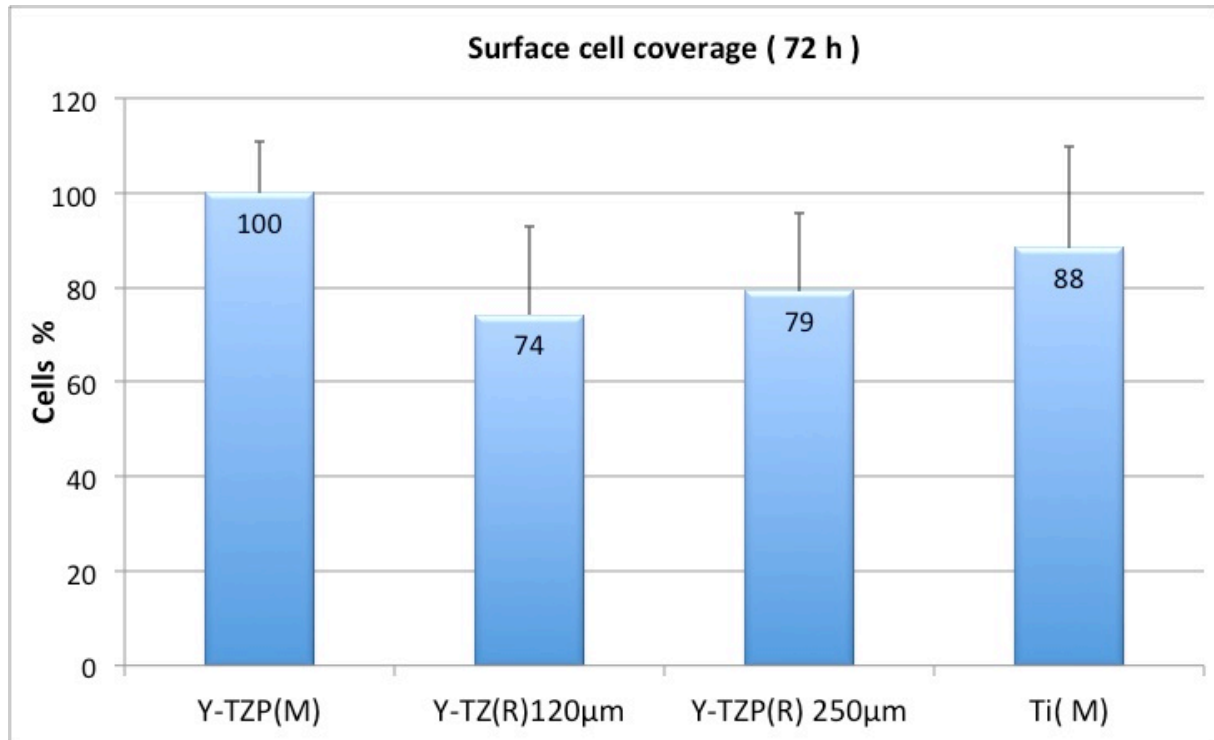


Figure 22: The means of three experiments of cell coverage and spreading after 72 h. determined by crystal violet staining are shown with standard deviations. Four samples were tested per group in each experiment (total n=12). Machined zirconia was used as a reference and set to 100%.

The combined data from three experiments (Fig. 22) show that the machined surfaces of zirconia and titanium after 72 h. show the higher percentage of SAOS-2 osteoblast cells.

The machined zirconia was set to (100%) as a reference surface. The percentage of cells on machined titanium was (88%). On roughened zirconia samples, the percentage of cell coverage was less (74% for samples sandblasted with 120 µm Al_2O_3 vs. 79% for the samples sandblasted with 250 µm Al_2O_3). See (Fig.23) for typical examples.

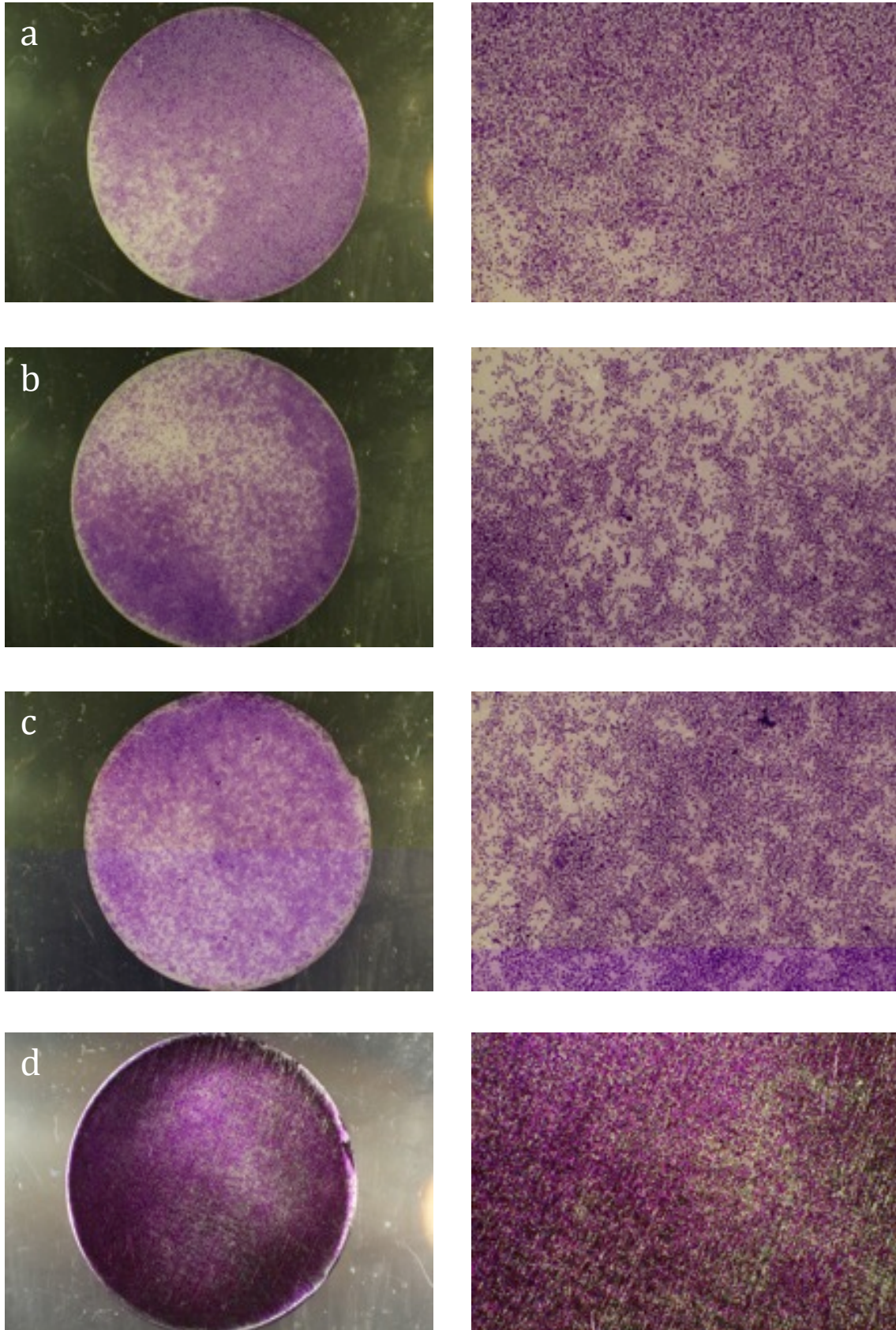


Figure 23: Photo-documentation of Crystal violet test after 72 h shows surface coverage by osteoblasts on different surfaces. (a) Machined zirconia sample, (b) zirconia sandblasted with 120 μm Al_2O_3 , (c) zirconia sandblasted with 250 μm Al_2O_3 , and (d) machined titanium.

3.3 Test of metabolic activity and proliferation

As described earlier, both tests were performed on the same samples consecutively; the result of the metabolic activity (XTT test) was obtained first, followed by the BrdU test. All surfaces were tested in three experiments.

In metabolic activity test XTT (Fig. 24) is graphical representation of one test from three tests, and the results of three tests are summarized in (Fig. 25). In proliferation test BrdU, (Fig. 26) is graphical representation of one from three tests, and the results of three tests are summarized in (Fig. 27).

3.3.1 metabolic activity (XTT assay)

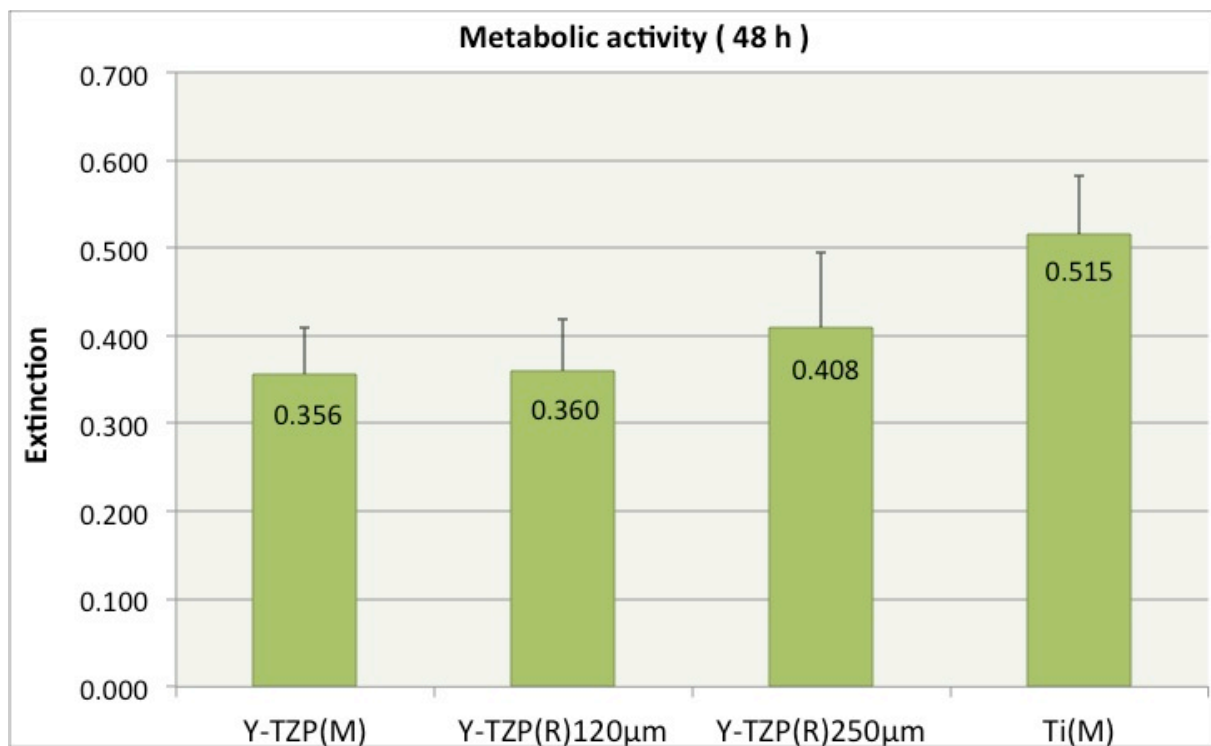


Figure 24: Metabolic activity of osteoblasts after 48 h. A typical experiment is shown. Bars represent means and S.D from four samples in each group. Metabolic activity was determined by the XTT assay and absorbance measured on an ELISA reader at 492 nm (reference wavelength: 620 nm).

In (Fig. 24,25) the metabolic activity of different zirconia samples was not significantly different, the machined surfaces of zirconia showed the extinction of (0.356) and for

samples sandblasted with ($120\ \mu\text{m}\ \text{Al}_2\text{O}_3$) was (0.360), and for the samples sandblasted with ($250\ \mu\text{m}\ \text{Al}_2\text{O}_3$) was (0.408). The machined titanium samples showed slightly higher extinction value (0.515).

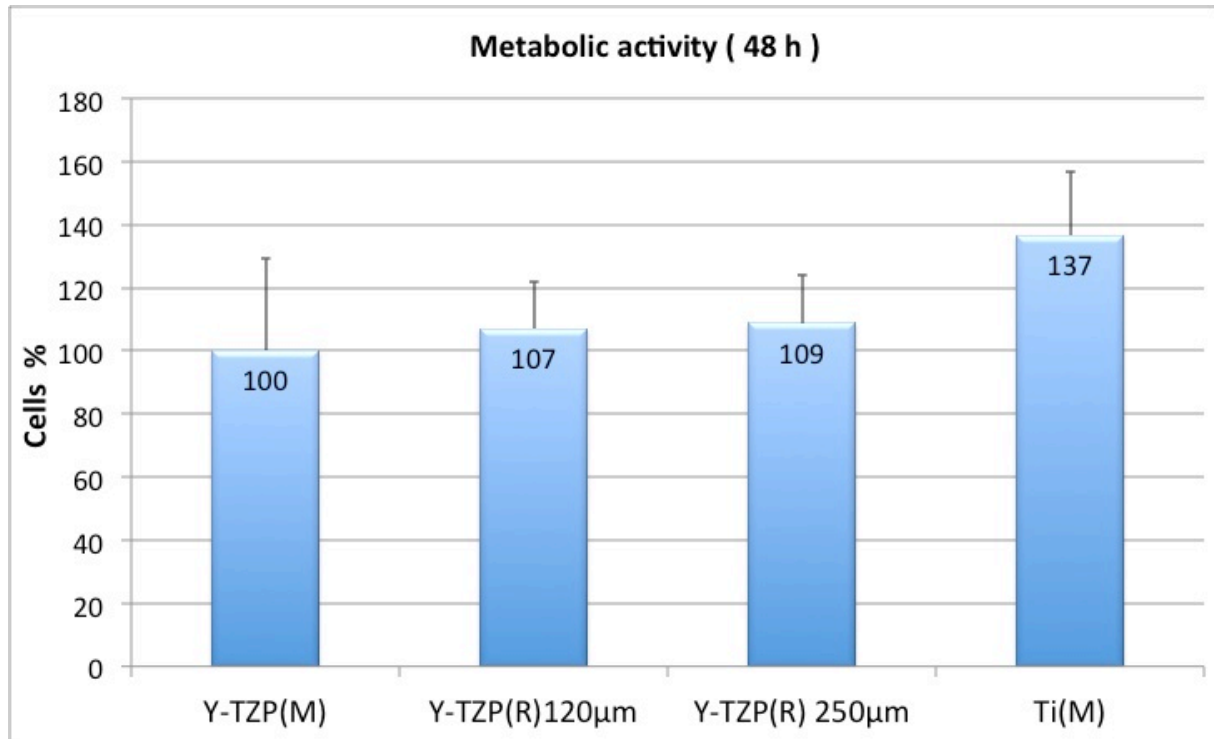


Figure 25: The means of three experiments of XTT assay are shown with standard deviations. Four samples were tested per group in each experiment (total $n=12$). Machined zirconia was used as a reference and set to 100%.

As shown in (Fig. 25) the metabolic activity of three experiments show slightly higher percentage of SAOS-2 osteoblast on machined titanium (137%), the results of the zirconia samples machined and roughened were similar and varied from 100% (set as reference for the machined surface), to (107%) sandblasted with $120\ \mu\text{m}\ \text{Al}_2\text{O}_3$ and (109 %) sandblasted with $250\ \mu\text{m}\ \text{Al}_2\text{O}_3$.

3.3.2 Proliferation test (BrdU assay)

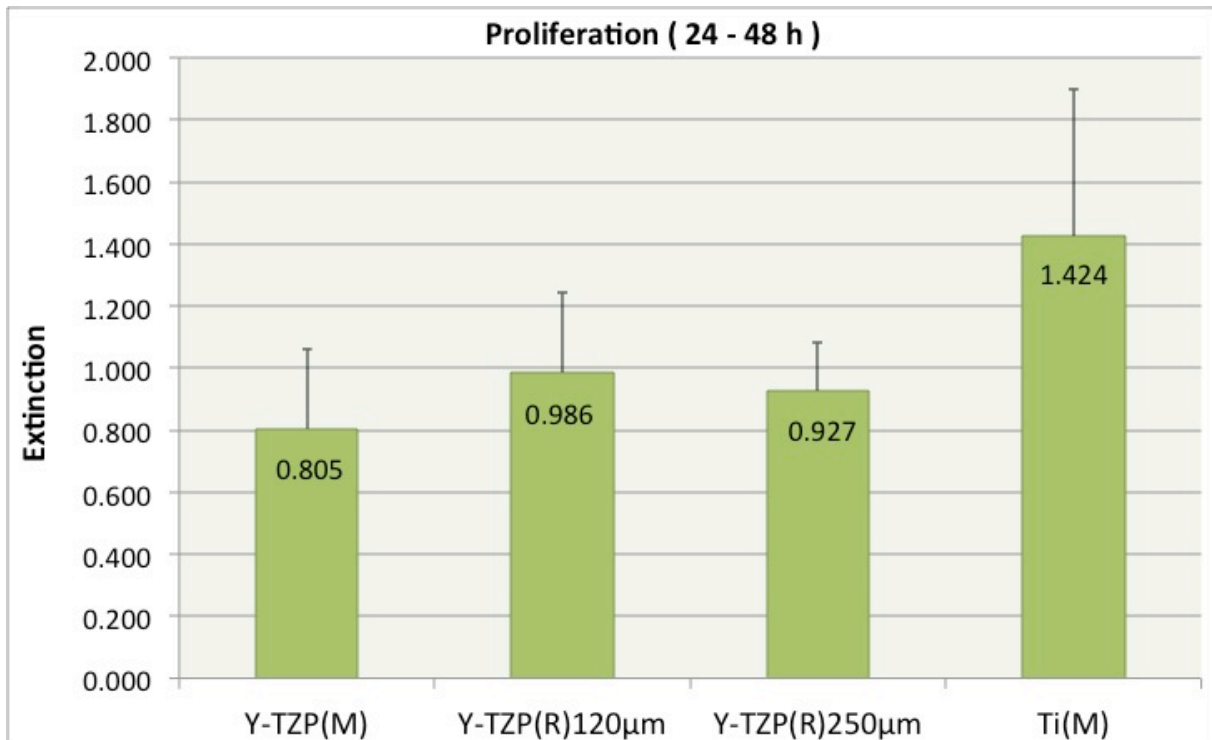


Figure 26: Osteoblast proliferation test after 24-48 h. A typical experiment is shown. Bars represent means and S.D. from four samples in each group. Proliferation was determined by the BrdU assay and absorbance measured on an ELISA reader at 450 nm (reference wavelength: 550 nm).

As shown in (Fig. 26,27) the proliferation rate of SAOS-2 osteoblasts determined by BrdU test revealed a higher extinction value compared to the others, Fig. (26) shows the result of a typical experiment. Fig. (27) shows the sum of three BrdU experiments.

The extinction value of machined titanium was (1.424) markedly higher than the zirconia samples. The extinction value of machined zirconia was (0.805), samples sandblasted with 120 µm Al_2O_3 was (0.986) and samples sandblasted with 250 µm Al_2O_3 was (0.927).

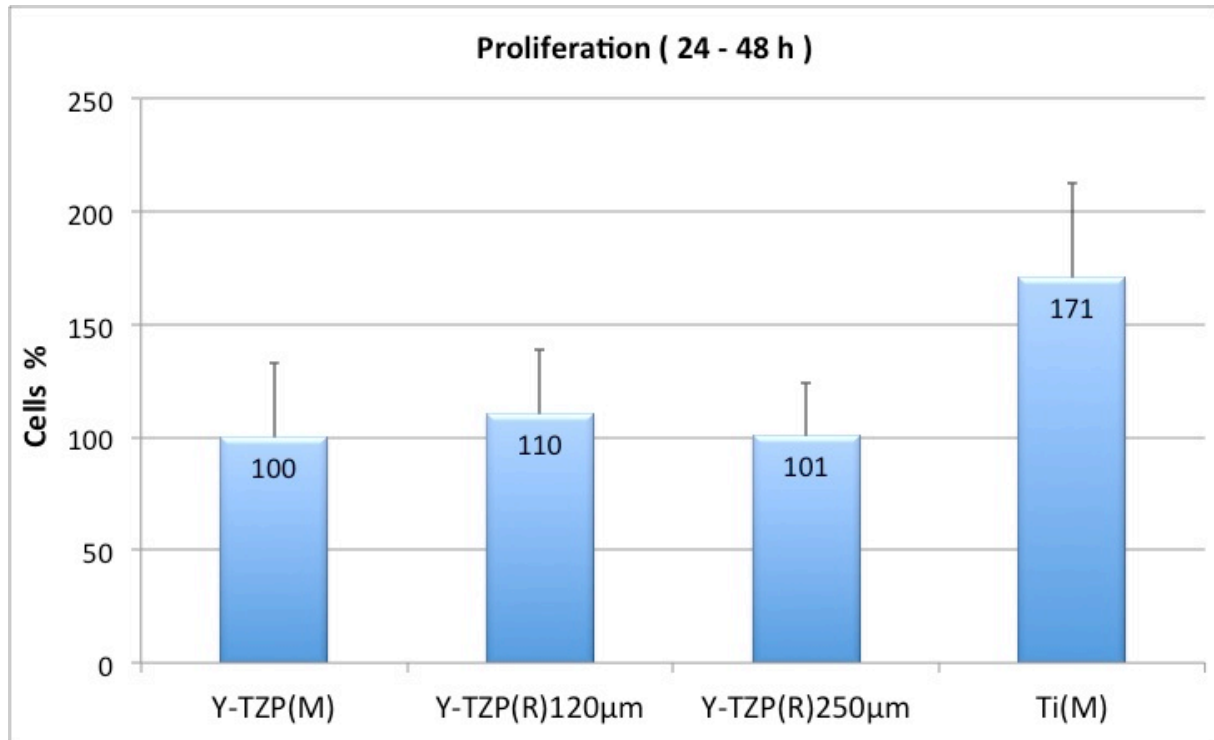


Figure 27: The means of three experiments of BrdU assay are shown with standard deviations. Four samples were tested per group in each experiment (total n=12). Machined zirconia was used as a reference and set to 100%.

In (Fig. 27), the combined data of three experiments determined by BrdU test confirmed that proliferation rate in log growth phase between 24-48 h. of SAOS-2 osteoblasts was higher on machined surfaces of titanium at percentage of (171%). On roughened zirconia samples, the proliferation was less (110 % for samples sandblasted with 120 µm Al_2O_3 vs. 101 % for the samples sandblasted with 250 µm Al_2O_3).

4.0 Discussion

In the present study, the cellular behavior of SAOS-2 osteoblasts was studied on two roughened zirconia surfaces compared to machined zirconia and titanium. This study highlights four important issues in the emerging field of cell-material interactions: cell adhesion, proliferation, metabolic activity, and cell coverage on different surface materials and structures.

The background of this in vitro study is to improve the design of zirconia implant surfaces. Studies and clinical experience with titanium as the base material have shown that the micro-morphological surface structure of an implant plays an important role in cell / surface interactions (Groessner-Schreiber and Tuan 1991; Anselme 2000). Numerous studies of titanium surfaces have shown that rough or porous surfaces play a major role in implant osteointegration (Kirsch and Donath 1984; Larsson et al. 1994; Martin et al. 1995; Wennerberg and Albrektsson 2009; Boyan et al. 1998; Lincks et al. 1998; Lohmann et al. 1999; Schwartz et al. 1999; Boyan et al. 1998).

The initial biomechanical interaction between cell and implant material plays a crucial role in the further interaction between tissue and material. The adhesion and proliferation of osteoblasts is important for the functional integration of an implant and is a key point for further proliferation and differentiation of the cells (Anselme 2000). Therefore, appropriate studies in cell culture systems are a first step in the evaluation of potential implant surfaces.

4.1 Surface topography and roughness

Topography was analyzed using a mechanical profile method (Perthometer). This method is able to detect and calculate the surface characteristics of a 9-mm² section for each sample. In the present study, both machined and rough surfaces underwent the same surface measurements. Although this experiment utilized manually controlled conditions and parameters for sandblasting, the process was adequate

and reproducible because of a special auxiliary technique used to control the process. Optically controlled removal of the colored surface by sandblasting with Al_2O_3 particles is considered a reliable method with acceptable standard deviations (Fig. 10). Nevertheless, roughening the zirconia surface manually and visually may be affected by a certain variation of process conditions.

Furthermore, the stylus method for studying the surface profile depth of sandblasted samples may not be optimal. The representations of the profile depth suggest that the tip did not record the ground of the surface completely due to the geometry, including the radius and angle of the needle's tip ($2\ \mu\text{m}$, 90°) and the speed of the scan ($0.5\ \text{mm/sec}$).

The original goal of this study was to prove that roughening the surface of pre-sintered zirconia specimens is a reliable and effective method for stimulating the osteoblast cells, which was achieved in this experiment. Another aspect to this experiment was the maintenance of the original physical properties of zirconia. Monaco et al. (2012) confirmed that the "abrasion ...(before sintering)... zirconia specimens resulted in rougher surfaces, and the monoclinic phase associated with the abrasion was completely transformed to the tetragonal state during the subsequent sintering step. In contrast, the sintered zirconia specimens resulted in surfaces with a lower roughness, a monoclinic phase, and compressive surface residual stresses, the degree of which was associated with the abrasive grain size" (Monaco et al. 2012).

The investigated surface was viewed carefully under the light microscope; the smooth machined zirconia surfaces had small scratches. These were probably made during the preparation of individual samples with a cutting wheel and could not be smoothed completely by the subsequent polishing process. Attention must be paid to clean the surface of the powder resulting from the cutting process by exposing each sample to a high-pressure air stream and then cleaning them with wet gauze. However, little scratches still appeared on the smooth samples. The results of the roughness analysis (section 3.1) confirmed the observations: the machined TZP specimen had a roughness of $0.27\ \mu\text{m}$. For the cell culture experiments, all samples were individually controlled by light microscopy and those with clear striations sorted

out and not used. The defective samples were replaced with new ones to maintain the intended number of discs in the experiment.

The samples sandblasted with 250 μm Al_2O_3 at two bar pressure exhibited irregularities on their surface edges. These irregularities were not avoidable because of the force reflected by the size of the sandblasted material. The discs sandblasted with 120 μm Al_2O_3 had very homogenous surfaces from the center of the samples until the edges, and the roughness was similar to the 250 μm Al_2O_3 sandblasted samples.

This experiment showed similarities in the surface roughness before and after sintering, and the shrinkage of sintered zirconia did not markedly affect the roughness values. The differences in sample roughness (sandblasted vs. machined) were reflected in the adhesion, spreading, proliferation, and metabolic activity results.

4.2 Cell culture model

Cell culture studies provide the starting point for assessing the biological responses to a material and have advantages over in vivo models, such as lower cost and standardized experimental conditions by which a better comparison of results can be achieved. However, a disadvantage of an in vitro study is that it is a static system in which the complexity of the processes cannot be considered as in experiments in vivo.

The osteoblast cell line used in this study came from a human osteogenic sarcoma (bone tumor). The use of these cells has both advantages and disadvantages. Some advantages of such a permanent cell line is unlimited availability with lower biological variance and the ease of use. However, the cells are derived from an osteosarcoma, so they can differ in appearance and behavior from primary cell cultures isolated directly from human tissue. In addition, cell lines created through transformation do not represent all properties of the original cell type. However, the SAOS-2 osteoblasts used here has been used in a number of previous studies (Anderson et al. 1992; Hunt, Schwappach, and Anderson 1996; Degasne et al. 1999; Okumura et al. 2001; Postiglione et al. 2003; Zhu et al. 2004).

Because this was an in vitro study, only the response of a single cell type was observed. Thus, the clinical relevance of the results has to be confirmed in further animal and clinical studies.

4.3 Effect of surface modification on cellular adhesion, spreading, metabolic activity, and proliferation

4.3.1 Cell adhesion and cell coverage (crystal violet assay)

Cell attachment is influenced by surface roughness as confirmed in numerous studies of adhesion and proliferation, differentiation, matrix synthesis, and growth factor production (reviewed by Borghetti et al. 2005). Most of these studies were on titanium surfaces. Lincks et al. (1998) concluded that roughness remains the overriding variable in promoting osteogenic differentiation and, on the nanometer scale, seems to affect cell orientation and migration. However, with increasing surface roughness, both the bone formation rate and the proportion of surface area in direct contact with the bone increases (Grössner-Schreiber and Tuan 1991; Cooper et al. 1999; Buser et al. 1991).

In the present in vitro experiment, the crystal violet test found that surface roughness increases cell adhesion. More cells adhered to zirconia samples sandblasted with 120 μm or 250 μm Al_2O_3 compared to machined titanium or zirconia surfaces. Although the difference in roughness between the sandblasted discs was minimal, more cells adhered to the more roughened zirconia discs (250 μm sandblasted).

Staining adherent cells with crystal violet is simple and easily done. Some bound cells may be lost due to washing steps. In addition, this method does not allow quantitation of cell number in reference to a standard curve. Changes in OD measure the qualitative variation in adhesion rather than the number of bound cells (Bellavite et al. 1992).

The cause of this increase can be assumed to be enlargement of the available surface with increasing surface roughness (Buser et al. 1999; Bowers et al. 1992; Qu,

Chehroudi, and Brunette 1996). In regards to cell behavior on titanium surfaces, roughness facilitates or enhances cell adhesion and spreading (Zhu et al. 2004). Another aspect of the crystal violet test is that it can indicate cell coverage, and in this study, the machined zirconia surface exhibited more spreading and coverage than the roughened zirconia samples and even the machined titanium surface.

4.3.2 Metabolic activity (XTT assay)

The XTT test was used to assess cell viability as a function of redox potential. Actively respiring cells convert the water-soluble XTT to a water-soluble orange-colored formazan product. The sensitivity of the XTT reduction assay has been reported to be similar to or better than that of the MTT reduction assay.

The metabolic activity was investigated after 48 h, showing comparable and similar results among the four tested groups. Therefore, the biocompatibility of zirconia is similar to that of titanium. Thus, the use of zirconia has no cytotoxic consequences on the SAOS-2 osteoblasts.

4.3.3 Cell proliferation (BrdU assay)

This test showed that cellular proliferation was better on titanium discs than on all zirconia discs. It has been demonstrated that osteoblasts do not spread completely on rough surfaces and acquire a polygonal morphology with a diminished cell proliferation rate (Sennerby et al. 2005). Despite the complexity of surface/bone tissue interactions in vivo, in vitro studies may provide relevant information about cell/biomaterial interactions and their mechanisms. For example, the effect of surface roughness is controverted because some studies indicate that cell proliferation increases on smoother surfaces (Anselme et al. 2000).

Zhang et al. (2012) studied the behavior of osteoblast-like cells on titanium and zirconia films deposited by cathodic arc deposition and found that cells on TiO₂ and ZrO₂ films have a polygonal shape and appear more spread out and flattened than on Ti disks. No obvious difference in cell morphology was observed between osteoblasts on TiO₂ and ZrO₂ films.

Thus, it can be assumed that osteoblasts respond in a comparable way to surface morphology on both materials, and that the clinical performance of zirconia implant surface can be optimized in a similar way as already known for titanium dental implants.

In vivo studies utilizing different animal models have concluded that there is currently sufficient evidence that titanium implants with micro-rough surfaces achieve faster bone integration, a higher percentage of bone implant contact, and a higher resistance to shear documented with higher removal torque values compared to titanium implants with a polished or machined surfaces.

Studies have shown that osteoblasts are sensitive to surface roughness, exhibiting decreased proliferation and a more differentiated phenotype on rougher surfaces. PGE2 production is enhanced on rough surfaces, as is the production of TGF beta 1, suggesting that surface roughness can mediate the autocrine and paracrine regulation of osteogenesis. Moreover, surface roughness modulates the effect of systemic hormones such as 1,25-(OH) 2D3 on osteoblasts (Nasatzky, Gultchin, and Schwartz 2003).

In recent clinical trials, Nasatzky et al. (2003) observed that rough implant surfaces have clinical advantages. In humans, roughened titanium implants (SLA and Osseotite) require shorter healing periods, 6-8 weeks instead of 12 weeks, before loading. In addition, certain roughened implants could be used at shorter sizes (6-8 mm). However, sufficient long-term documentation is still lacking, and the predictability of such modalities has yet to be examined in long-term prospective clinical trials (Nasatzky, Gultchin, and Schwartz 2003). In contrast, biomechanical and histomorphometrical investigations of zirconia implants are very rare in the literature.

Sennerby et al. (2005) demonstrated a strong bone tissue response to surface-modified zirconia implants in rabbit bone. Implants were placed in the tibia and femur of 12 rabbits. The RTQ results showed higher values for zirconia implants with two different porous structures than for the titanium implants (Nobel Biocare, Goteborg, Sweden) after a healing period of 6 weeks. However, the lowest values were

measured for the machined zirconia implants. No significant differences regarding bone-to-implant contact and bone area filling were observed between the different treatment groups (Sennerby et al. 2005).

5.0 Conclusions and outlook

The results of the present study indicate that sandblasting the zirconia surface before sintering is a suitable method for surface roughening. The initial cell adhesion of osteoblasts was enhanced up to 175% compared to the machined zirconia reference. The surface cell coverage after prolonged incubation (72 h) was markedly decreased on the roughened samples. This may indicate the shift of the osteoblast cells towards differentiation, induced by surface roughness. In addition, the metabolic activity and proliferation in logarithmic growth phase (24-48) were not affected.

Basically, the roughness procedure increases the surface area of the implant, the surface modification technique investigated here (sandblasting before sintering) allows manufacturing of zirconia implants with varying surface roughness without affecting the mechanical strength, a roughened surface was evident on the sandblasted specimens in both surface roughness analysis and SEM images. Different grain-sized sandblasting materials should be tested in further studies to determine their influence on cell behavior.

This work represents a promising concept, however; the initial results should be reviewed and built on in further studies.

6.0 Summary

The surface structure of the implant plays a crucial role in the success of implantation. Therefore, the surfaces of dental implants have been under continuous development over the past few decades. In zirconia implants, generating surface roughness by sandblasting may induce surface damage and phase transformation from tetragonal to monoclinic phase. To avoid these negative effects, sandblasting prior to sintering is one strategy to generate a rough zirconia surface.

The aim of this study was to investigate the influence of surface roughening zirconia base material, TZP, by sandblasting prior to sintering process under defined parameters. The new surface structure was then examined in vitro on the basis of cellular adhesion (after 60 min with crystal violet), cell coverage (after 72 h with crystal violet), proliferation and metabolic activity (24-48 h with BrdU assay and after 48 h with XTT assay, respectively) of human SAOS-2 osteoblasts.

Using a Perthometer, the roughened zirconia variants exhibited negligible changes in surface roughness before and after sintering, and they maintained their original mechanical properties by avoiding post-treatment of the surfaces. Initial cell adhesion was positively enhanced by a roughened surface compared to a machined surface. The metabolic activity and proliferation in the log-growth phase were not affected. Surface coverage by cells was slightly decreased on rough zirconia surfaces compared to the machined reference; however, surface coverage on all zirconia surfaces was comparable to that of titanium, indicating good biocompatibility. Therefore, the method used to roughen the zirconia surface in this experiment is suitable for zirconia implants, which is an alternative implant material.

Sandblasting before sintering zirconia implants is an appropriate method to create surface roughness without compromising the mechanical strength.

7.0 Literature

- Adell R, Eriksson B, Lekholm U, Brånemark PI, Jemt T. 1990. "Long-Term Follow-up Study of Osseointegrated Implants in the Treatment of Totally Edentulous Jaws." *The International Journal of Oral Maxillofacial Implants* 5: 347–359.
- Albrektsson T, Hansson HA, Ivarsson B. 1985. "Interface Analysis of Titanium and Zirconium Bone Implants." *Biomaterials* 6: 97–101.
- Albrektsson T, Wennerberg A. 2004. "Oral Implant Surfaces : Part 1 — Review Focusing on Topographic and Chemical Properties of Different Surfaces and In Vivo Responses to Them Aspects of Surface Quality." *International Journal of Prosthodontics* 17: 536–543.
- Anderson HC, Sugamoto K, Morris DC, Hsu HH, Hunt T. 1992. "Bone-Inducing Agent (BIA) from Cultured Human Saos-2 Osteosarcoma Cells." *Bone and Mineral* 16: 49–62.
- Anselme K, 2000. "Osteoblast Adhesion on Biomaterials." *Biomaterials* 21: 667–681.
- Anselme K, Bigerelle M, Noel B, Dufresne E, Judas D, Iost A, Hardouin P. 2000. "Qualitative and Quantitative Study of Human Osteoblast Adhesion on Materials with Various Surface Roughnesses." *Journal of Biomedical Materials Research* 49: 155–166.
- Bellavite P, Chirumbolo S, Mansoldo C, Gandini G, Dri P. 1992. "Simultaneous Assay for Oxidative Metabolism and Adhesion of Human Neutrophils: Evidence for Correlations and Dissociations of the Two Responses." *Journal of Leukocyte Biology* 51: 329–335.
- Borghetti P, De Angelis E, Caldara G, Corradi A, Cacchioli A, and Gabbi. 2005. "Adaptive Response of Osteoblasts Grown on a Titanium Surface: Morphology, Cell Proliferation and Stress Protein Synthesis." *Vet Res Commun* 29: 221–24.
- Boudrias P, Shoghikian E, Morin E, Hutnik P.. 2001. Esthetic Option for the Implant-Supported Single-Tooth Restoration - Treatment Sequence with a Ceramic Abutment., *67 Journal Canadian Dental Association* 508–514.
- Bowers KT, Keller JC, Randolph BA, Wick DG, Michaels CM. 1992. "Optimization of Surface Micromorphology for Enhanced Osteoblast Responses in Vitro." *The International Journal of Oral & Maxillofacial Implants* 7: 302–310.
- Boyan BD, Batzer R, Kieswetter K, Liu Y, Cochran DL, Szmuckler-Moncler S, Dean DD, Schwartz Z.. 1998. "Titanium Surface Roughness Alters Responsiveness of MG63 Osteoblast-like Cells to 1 alpha,25-(OH)2D3." *Journal of Biomedical Materials Research* 39: 77 – 85.
- Boyan BD, Lossdörfer S, Wang L, Zhao G, Lohmann CH, Cochran DL, Schwartz Z. 2003. "Osteoblasts Generate an Osteogenic Microenvironment When Grown on Surfaces with Rough Microtopographies." *European Cells & Materials* 6: 22–27.

- Brodbeck, U. 2003. "The ZiReal post:A New Ceramic Implant Abutment." *Esthet.Restor.Dent.* 15: 10–23.
- Buser D, Nydegger T, Oxland T, Cochran DL, Schenk RK, Hirt HP, Snétivy D, Nolte LP.. 1999. "Interface Shear Strength of Titanium Implants with a Sandblasted and Acid-Etched Surface: A Biomechanical Study in the Maxilla of Miniature Pigs." *Journal of Biomedical Materials Research* 45: 75–83.
- Buser D, Schenk RK, Steinemann S, Fiorellini JP, Fox CH, Stich H. 1991. "Influence of Surface Characteristics on Bone Integration of Titanium Implants. A Histomorphometric Study in Miniature Pigs." *Journal of Biomedical Materials Research* 25: 889–902.
- Christel P, Meunier A, Dorlot J-M et al. 1988. "Biomechanical Compatibility and Design of Ceramic Implants for Orthopaedic Surgery. Bioceramics: Material Characteristics versus in Vivo Behavior." *Ann NY Acad Sci* 523: 234–56.
- Cooper LF, Masuda T, Whitson SW, Yliheikkilä P, Felton DA. 1999. "Formation of Mineralizing Osteoblast Cultures on Machined, Titanium Oxide Grit-Blasted, and Plasma-Sprayed Titanium Surfaces." *The International Journal of Oral & Maxillofacial Implants* 14 (1): 37–47.
- De Wijs FL, Van Dongen RC, De Lange GL, De Putter C. 1994. "Front Tooth Replacement with Tubingen (Frialit) Implants." *Journal of Oral Rehabilitation* 21: 11–26.
- Degasne I, Baslé MF, Demais V, Huré G, Lesourd M, Grolleau B, Mercier L, Chappard D. 1999. "Effects of Roughness, Fibronectin and Vitronectin on Attachment, Spreading, and Proliferation of Human Osteoblast-like Cells (Saos-2) on Titanium Surfaces." *Calcified Tissue International* 64: 499–507.
- Larsson C, Thomsen P, Lausmaa J, Rodahl M, Kasemo B, Ericson LE. 1994. "Bone Response to Surface Modified Titanium Implants: Studies on Electropolished Implants with Different Oxide Thicknesses and Morphology." *Biomaterials*.
- Geis-Gerstorfer J, Faessler P. 1999. "Untersuchungen Zum Ermüdungsverhalten Der Dentalkeramiken Zirkondioxid-TZP Und In-Ceram." *Dtsch Zahnärztl Z* 54: 692–694.
- Gahlert M, Gudehus T, Eichhorn S, Steinhauser E, Kniha H, Erhardt W. 2007. "Biomechanical and Histomorphometric Comparison between Zirconia Implants with Varying Surface Textures and a Titanium Implant in the Maxilla of Miniature Pigs." *Clinical Oral Implants Research* 18 (5) (October): 662–8.
- Gahlert M, Roehling S, Sprecher CM, Kniha H, Milz S, Bormann K. 2012. "In Vivo Performance of Zirconia and Titanium Implants: A Histomorphometric Study in Mini Pig Maxillae." *Clinical Oral Implants Research* 23: 281–6.
- Goff J. P, Hayes W, Hull S, Hutchings M. T, and Clausen K. N. 1999. "Defect Structure of Yttria-Stabilized Zirconia and Its Influence on the Ionic Conductivity at Elevated Temperatures." *Physical Review B* 59: 14202–14219.
- Grössner-Schreiber B, Tuan R S. 1991. "The Influence of the Titanium Implant Surface on the Process of Osseointegration." *Deutsche Zahnärztliche Zeitschrift* 46: 691–693.

- Hamilton DW, Brunette DM. 2007. "The Effect of Substratum Topography on Osteoblast Adhesion Mediated Signal Transduction and Phosphorylation." *Biomaterials* 28: 1806–1819.
- Helmer JD, Driskell TD. 1969. "Research on Bioceramics. Symp. on Use of Ceramics as Surgical Implants. South Carolina (USA)". Clemson University.
- Hempel U, Hefti T, Kalbacova M, Wolf-Brandstetter C, Dieter P, Schlottig F. 2010. "Response of Osteoblast-like SAOS-2 Cells to Zirconia Ceramics with Different Surface Topographies." *Clinical Oral Implants Research* 21 (2) (February): 174–81.
- Heydecke G, Kohal R, Gläser R. 1999. "Optimal Esthetics in Single-Tooth Replacement with the Re-Implant System: A Case Report." *The International Journal of Prosthodontics* 12 (2): 184–9.
- Hunt TR, Schwappach JR, Anderson HC. 1996. "Healing of a Segmental Defect in the Rat Femur with Use of an Extract from a Cultured Human Osteosarcoma Cell-Line (Saos-2). A Preliminary Report." *The Journal of Bone and Joint Surgery. American Volume* 78: 41–48.
- Ichikawa Y, Akagawa Y, Nikai H, Tsuru H. 1992. "Tissue Compatibility and Stability of a New Zirconia Ceramic in Vivo." *The Journal of Prosthetic Dentistry* 68: 322–326.
- Jones M, McColl I.R, Grant D.M, Parker K.G, and Parker T.L. 1999. "Haemocompatibility of DLC and TiC–TiN Interlayers on Titanium." *Diamond and Related Materials*. 52:457-462
- Kasemo B, Lausmaa J. 1988. "Biomaterial and Implant Surfaces: A Surface Science approach." 3(4):247-59
- Kelly JR, Denry I. 2008. "Stabilized Zirconia as a Structural Ceramic: An Overview." *Dental Materials Official Publication of the Academy of Dental Materials* 24: 289–298.
- Kim JB, Leucht P, Luppen CA, Park YJ, Beggs HE, Damsky CH, Helms JA. 2007. "Reconciling the Roles of FAK in Osteoblast Differentiation, Osteoclast Remodeling, and Bone Regeneration." *Bone* 41 (1) (July): 39–51.
- Kirschn A, Donath K 1984. "Tierexperimentelle Untersuchungen Zur Bedeutung Der Mikromorphologie von Titanimplantatoberflächen." *Fortschr Zahnärztl Implantol* I: 35–40.
- Kohal RJ, Klaus G. 2004. A Zirconia Implant-Crown System: A Case Report., 24 *The International journal of periodontics restorative dentistry* 147–153.
- Kohal RJ, Papavasiliou G, Kamposiora P, Tripodakis A, Strub JR. 2002. "Three-Dimensional Computerized Stress Analysis of Commercially Pure Titanium and Yttrium-Partially Stabilized Zirconia Implants." *The International Journal of Prosthodontics* 15: 189–194.
- Koutayas SO, Kern M 1999. "All-Ceramic Posts and Cores: The State of the Art." *Quintessence International Berlin Germany* 1998 30: 383–392.

- Kubies D, Himmlová L, Riedel T, Chánová E, Balík K, Douděrová M, Bártová J, Pešáková V. 2011. "The Interaction of Osteoblasts with Bone-Implant Materials: 1. The Effect of Physicochemical Surface Properties of Implant Materials." *Physiological Research / Academia Scientiarum Bohemoslovaca* 60 (1) (January): 95–111.
- Lincks J, Boyan BD, Blanchard CR, Lohmann CH, Liu Y, Cochran DL, Dean DD, Schwartz Z. 1998. "Response of MG63 Osteoblast-like Cells to Titanium and Titanium Alloy Is Dependent on Surface Roughness and Composition." *Biomaterials* 19: 2219–2232.
- Lohmann CH, Sagun R Jr, Sylvia VL, Cochran DL, Dean DD, Boyan BD, Schwartz Z 1999. "Surface Roughness Modulates the Response of MG63 Osteoblast-like Cells to 1,25-(OH)₂D₃ through Regulation of Phospholipase A₂ Activity and Activation of Protein Kinase A." *Journal of Biomedical Materials Research* 47: 139–151.
- Lutolf MP, Hubbell JA. 2005. "Synthetic Biomaterials as Instructive Extracellular Microenvironments for Morphogenesis in Tissue Engineering." *Nature Biotechnology* 23: 47–55.
- Martin JY, Schwartz Z, Hummert TW, Schraub DM, Simpson J, Lankford J Jr, Dean DD, Cochran DL, Boyan BD. 1995. "Effect of Titanium Surface Roughness on Proliferation, Differentiation, and Protein Synthesis of Human Osteoblast-like Cells (MG63)." *Journal of Biomedical Materials Research* 29: 389–401.
- Nasatzky E, Gultchin J, Schwartz Z. 2003. "The Role of Surface Roughness in Promoting Osteointegration." *Refuat Hapeh Vehashinayim* 20(3): 8–19, 98.
- Okumura A, M Goto, T Goto, M Yoshinari, S Masuko, T Katsuki, and T Tanaka. 2001. "Substrate Affects the Initial Attachment and Subsequent Behavior of Human Osteoblastic Cells (Saos-2)." *Biomaterials* 22: 2263–2271.
- Oliva X, Oliva J, Oliva JD. 2010. Full-Mouth Oral Rehabilitation in a Titanium Allergy Patient Using Zirconium Oxide Dental Implants and Zirconium Oxide Restorations. A Case Report from an Ongoing Clinical Study., 5 *The European journal of esthetic dentistry official journal of the European Academy of Esthetic Dentistry* 5:190–203.
- Payer M, Lorenzoni M, Jakse N, Kirmeier R, Dohr G, Stopper M, Pertl C. 2010. "Cell Growth on Different Zirconia and Ti-Tanium Surface Textures : A Morphologic in Vitro Study" 26(4):338-351.
- Piconi C, and Maccauro G. 1999. "Zirconia as a Ceramic Biomaterial." *Biomaterials* 20: 1–25.
- Pilathadka S, D Vahalová, and T Vosáhlo. 2007. "The Zirconia: A New Dental Ceramic Material. An Overview." *Prague Medical Report* 108: 5–12.
- Postiglione L, Di Domenico G, Ramaglia L, Montagnani S, Salzano S, Di Meglio F, Sbordone L, Vitale M, Rossi G. 2003. "Behavior of SaOS-2 Cells Cultured on Different Titanium Surfaces." *Journal of Dental Research* 82: 692–696.
- Puleo DA, Nanci A. 1999. "Understanding and Controlling the Bone-Implant Interface." *Biomaterials* 20 (23-24) (December): 2311–21.

- Qu J, Chehroudi B, Brunette DM. 1996. "The Use of Micromachined Surfaces to Investigate the Cell Behavioural Factors Essential to Osseointegration." *Oral Diseases* 2: 102–115.
- Ruff O, Ebert F, Stephen E. 1929. "Contributions to the Ceramics of Highly Refractory Materials. II. The System: Zirconia-Lime." *System Zirconialime* 180: 215–224.
- Schulte W. 1984. "The Intraosseous Al₂O₃ (Frialit)tuebingen implant.Developmental Status after Eight Years." *Quintessence Int* 15: 1–39.
- Schwartz Z, Lohmann CH, Oefinger J, Bonewald LF, Dean DD, Boyan BD. 1999. "Implant Surface Characteristics Modulate Differentiation Behavior of Cells in the Osteoblastic Lineage." *Advances in Dental Research* 13: 38–48.
- Schwartz Z, Nasazky E, Boyan BD.2005. "Surface Microtopography Regulates Osteointegration: The Role of Implant Surface Microtopography in Osteointegration." *The Alpha Omegan* 98: 9–19.
- Scudiero DA, Shoemaker RH, Paull KD, Monks A, Tierney S, Nofziger TH, Currens MJ, Seniff D, Boyd MR. 1988. "Evaluation of a Soluble Tetrazolium/formazan Assay for Cell Growth and Drug Sensitivity in Culture Using Human and Other Tumor Cell Lines." *Cancer Research* 48: 4827–4833.
- Sennerby L, Dasmah A, Larsson B, Iverhed M. 2005. "Bone Tissue Responses to Surface-Modified Zirconia Implants: A Histomorphometric and Removal Torque Study in the Rabbit." *Clinical Implant Dentistry and Related Research* 7 Suppl 1: 13–20.
- Silva, Viviane V, Fernando S Lameiras, and Zélia I P Lobato. 2002. "Biological Reactivity of Zirconia-Hydroxyapatite Composites." *Journal of Biomedical Materials Research* 63: 583–590.
- Sturzenegger B, Feher A, Lüthy H, Schumacher M, Loeffel O, Filser F, Kocher P, Gauckler L, Schärer P. 2000. "Klinische Studie von Zirkonoxid- Brücken Im Seitenzahnggebiet Hergestellt Mit Dem DCM-System." *Acta Med Dent Helv*, 5(12): 131–139.
- Subbarao, E.C.1981. "Zirconia—an Overview. In: Heuer AH, Hobbs LW, Editors. *Advances in Ceramics*." *Science and Techno-Logy of Zirconia*.3:1-24
- Sun F, Zhang GR, Zhang F, Liu F, Mao H, Huang L, Wang PF.2006. [The Use of CAD/CAM System with Zirconia in Modern Prosthodontics]. *Shanghai Kou Qiang Yi Xue. Journal of Stomatology* ;15(4):337-44.
- Monaco C, Tucci A, Esposito L, Scotti R. 2012. "Microstructural Changes Produced by Abrading Y-TZP in Presintered and Sintered Conditions" 1: 2–7.
- Wennerberg A. 1996 *On Surface Roughness and Implant Incorporation* [thesis]. Göteborg, Sweden: Department of Biomaterials, University of Goteborg :1–196.
- Wennerberg A, Albrektsson T. 2009. "Effects of Titanium Surface Topography on Bone Integration: A Systematic Review." *Clin Oral Implants Res* 20 Suppl 4 (September): 172–184.

- Zhang S, Sun J, Xu Y, Qian S, Wang B, Liu F, Liu X. 2012. "Biological Behavior of Osteoblast-like Cells on Titania and Zirconia Films Deposited by Cathodic Arc Deposition." *Biointerphases* 7 (1-4) (December): 60.
- Zhu X, Chen J, Scheideler L, Altebaeumer T, Geis-Gerstorfer J, Kern D. 2004. "Cellular Reactions of Osteoblasts to Micron- and Submicron-Scale Porous Structures of Titanium Surfaces." *Cells, Tissues, Organs* 178: 13–22.

8.0 Appendix

8.1 Results of surface roughness in the actual test

The difference in surface roughness before and after the sintering process was minimal. However, the average surface roughness was less after the sintering process than before the process (Tables 7-12). Ten samples were randomly selected from each group (machined and sandblasted with different sizes of Al_2O_3 particles) before and after sintering.

Machined zirconia discs (before sintering)

Table 7: Surface roughness of 10 randomized samples out of 50 samples of machined zirconia Roughness analysis carried out before the sintering procedure.

Sample	$R_a, \mu\text{m}$	$R_{\text{max}}, \mu\text{m}$	$R_z, \mu\text{m}$	$R_q, \mu\text{m}$	$R_p, \mu\text{m}$	$R_t, \mu\text{m}$
1	0.38	3.38	2.60	0.49	1.10	3.44
2	0.23	2.06	1.61	0.30	0.83	2.14
3	0.43	4.39	3.04	0.58	1.15	4.70
4	0.25	2.15	1.71	0.32	0.90	2.23
5	0.23	1.89	1.53	0.29	0.78	1.98
6	0.48	3.88	2.97	0.60	1.44	3.94
7	0.28	2.23	1.84	0.34	0.90	2.33
8	0.38	3.11	2.63	0.49	1.20	3.45
9	0.19	1.75	1.39	0.24	0.67	1.83
10	0.26	2.11	1.85	0.33	0.87	2.20
Mean	0.31	2.69	2.12	0.40	0.98	2.82
S.D	0.04	0.41	0.27	0.05	0.12	0.43

Machined zirconia discs (after sintering)

Table 8: Surface roughness of 10 randomized samples out of 50 samples of machined zirconia. Roughness analysis carried out after the sintering procedure.

Sample	$R_a, \mu\text{m}$	$R_{\text{max}}, \mu\text{m}$	$R_z, \mu\text{m}$	$R_q, \mu\text{m}$	$R_p, \mu\text{m}$	$R_t, \mu\text{m}$
1	0.34	3.13	2.40	0.44	1.18	3.30
2	0.23	2.22	1.73	0.30	0.93	2.31
3	0.23	2.45	1.79	0.30	1.02	2.56
4	0.23	2.13	1.68	0.29	0.91	2.23
5	0.29	2.55	2.00	0.36	1.06	2.68
6	0.43	4.51	3.06	0.57	1.63	4.68
7	0.22	2.12	1.64	0.28	0.89	2.21
8	0.36	3.15	2.48	0.47	1.23	3.35
9	0.13	1.69	1.18	0.18	0.69	1.78
10	0.22	2.15	1.73	0.29	0.92	2.25
Mean	0.27	2.61	1.97	0.35	1.05	2.74
S.D	0.09	0.81	0.54	0.11	0.26	0.84

120 μm Al_2O_3 with 2-bar pressure (before sintering)

Table 9: Surface roughness of 10 randomized zirconia samples out of 50 samples sandblasted with 120 μm Al_2O_3 . Roughness analysis carried out before the sintering procedure.

Sample	$R_a, \mu\text{m}$	$R_{\text{max}}, \mu\text{m}$	$R_z, \mu\text{m}$	$R_q, \mu\text{m}$	$R_p, \mu\text{m}$	$R_t, \mu\text{m}$
1	3.22	22.39	18.04	4.03	8.38	23.51
2	3.19	22.16	17.68	4.00	8.32	23.22
3	3.13	21.44	17.28	3.92	8.04	22.57
4	3.04	21.10	16.99	3.81	7.85	22.01
5	3.15	22.03	17.57	3.97	8.20	23.02
6	3.06	21.06	17.25	3.84	7.94	22.21
7	3.12	22.24	17.54	3.94	8.17	23.20
8	2.95	20.75	16.53	3.70	7.76	21.82
9	3.15	22.00	17.56	3.96	8.21	23.13
10	3.21	22.09	17.84	4.02	8.28	23.31
Mean	3.17	21.85	17.65	3.98	8.26	23.01
S.D	0.39	3.36	2.10	0.49	1.05	3.38

125 μm Al_2O_3 with 2-bar pressure (after sintering)

Table 10: Surface roughness of 10 randomized zirconia samples out of 50 samples sandblasted with 120 μm Al_2O_3 . Roughness analysis carried out after the sintering procedure.

Sample	R_a , μm	R_{max} , μm	R_z , μm	R_q , μm	R_p , μm	R_t , μm
1	2.89	19.84	16.22	3.61	7.56	20.75
2	2.99	21.02	16.94	3.75	7.81	21.92
3	2.87	19.92	16.34	3.60	7.62	20.77
4	2.97	20.53	16.92	3.73	7.81	21.47
5	3.00	21.02	17.15	3.76	8.01	21.98
6	2.92	20.66	16.83	3.67	7.84	21.87
7	3.01	20.71	16.99	3.77	7.82	21.68
8	3.02	21.24	17.12	3.79	8.02	22.13
9	2.90	20.42	16.62	3.64	7.67	21.27
10	2.90	20.59	16.61	3.65	7.67	21.55
Mean	2.95	20.60	16.77	3.70	7.78	21.54
S.D	0.06	0.45	0.32	0.07	0.15	0.49

250 μm Al_2O_3 with 2-bar pressure (before sintering)

Table 11: Surface roughness of 10 randomized zirconia samples out of 50 samples sandblasted with 250 μm Al_2O_3 . Roughness analysis carried out before the sintering procedure.

Sample	$R_a, \mu\text{m}$	$R_{\text{max}}, \mu\text{m}$	$R_z, \mu\text{m}$	$R_q, \mu\text{m}$	$R_p, \mu\text{m}$	$R_t, \mu\text{m}$
1	4.30	30.58	23.62	5.45	10.74	32.28
2	3.91	27.41	21.62	4.94	10.06	29.06
3	3.88	27.92	21.49	4.93	10.06	29.31
4	4.00	28.42	22.02	5.07	10.35	30.05
5	4.02	28.73	21.89	5.09	10.13	29.95
6	4.05	28.29	22.02	5.10	10.56	29.52
7	3.86	27.11	21.23	4.89	9.93	28.58
8	3.98	28.30	21.80	5.03	10.13	29.85
9	4.21	29.46	23.00	5.31	10.91	31.03
10	3.85	26.46	20.82	4.85	9.90	27.91
Mean	4.01	28.27	21.95	5.07	10.28	29.75
S.D	0.15	1.18	0.82	0.19	0.35	1.23

250 μm Al_2O_3 with 2-bar pressure (after sintering)**Table 12: Surface roughness of 10 randomized zirconia samples out of 50 samples sandblasted with 250 μm Al_2O_3 . Roughness analysis carried out after the sintering procedure.**

Sample	$R_a, \mu\text{m}$	$R_{\text{max}}, \mu\text{m}$	$R_z, \mu\text{m}$	$R_q, \mu\text{m}$	$R_p, \mu\text{m}$	$R_t, \mu\text{m}$
1	4.05	28.37	22.32	5.11	10.23	29.73
2	3.74	26.20	20.53	4.71	9.82	27.39
3	3.83	26.44	20.75	4.80	9.91	27.69
4	3.72	25.98	20.74	4.69	9.94	27.16
5	3.86	27.34	21.34	4.86	10.06	28.56
6	3.99	27.41	21.65	5.00	10.20	28.62
7	3.78	26.30	20.52	4.74	9.80	27.33
8	3.87	26.26	21.06	4.84	9.99	27.61
9	3.90	28.15	21.41	4.93	10.17	29.25
10	3.80	27.05	20.82	4.80	9.74	28.38
Mean	3.86	26.95	21.11	4.85	9.99	28.17
S.D	0.11	0.85	0.57	0.13	0.17	0.87

Acknowledgment

I would like to express the deepest appreciation and thanks to Professor Jürgen Geis-Gerstorfer, for his genius ideas, support, enthusiastic encouragement and valuable suggestions during the planning and development of my dissertation.

My special appreciation and thanks to my advisor and supervisor Dr. Lutz Scheideler, for his excellent supervision, encouragement, great advises, useful critiques of this dissertation.

My deepest gratitude to Mrs. Christine Schille, for the discussions that helped me sort out the technical details of surface roughness and topography. She has been always there to listen and give advices.

I would especially like to thank Mrs. Cornelia Füger, for her encouragement and practical advices in biological laboratory.

I would also like to extend my thanks to all members of the department of Medical Materials and Technology, in Tübingen University hospital with whom I have interacted during my research work. Particularly, Mr. Schweizer Ernst and Mr. Spintzyk Sebastian, for their help and technical support to accomplish my dissertation.

Finally, I thank my family for their support and encouragement throughout my study, especially my wife and my kids.

Curriculum vitae

Name: Al-Qahtani Waleed Mohammed S

Date of birth: 20.01.1977

Gender: Male

Marital status: Married

Children: 2

Education and Qualifications

2000/2001 Bachelor in Dental Medicine & Surgery from King Abdulaziz University (KAU).

2001-2002 Internship program in department of prosthodontics and implantology.

2006 Toefl IBT (Total score: 103).

2009 German language (B 2.2 level).

2009-2010 Postgraduate program in Prosthodontics and Periodontology, Freiburg University.

2010-2014 Postgraduate program in Prosthodontics and Implantology, Tübingen University.

Science activity:

08.09 2013 Poster presentation of (Influence of sandblasting before sintering on flexural strength of Y-TZP Zirconia) at German dentists day in Frankfurt.

15.06.2014 Poster publication (Influence of sandblasting before sintering on flexural strength of Y-TZP Zirconia) International Poster Journal in Dentistry and Oral Medicine.

